COLLOIDAL GEL AND ITS APPLICATION IN TISSUE ENGINEERING

By

BAOJUN XIE

Master of Science

Oklahoma State University

Stillwater, Oklahoma

2003

Submitted to the Faculty of the
Graduate College of the
Oklahoma State University
in partial fulfillment of
the requirements for
the degree of
DOCTOR of PHILOSOPHY
December, 2005

COLLOIDAL GEL AND ITS APPLICATION

IN TISSUE ENGINEERING

Thesis Approved:

James E. Smay

Thesis Advisor

AJ Johannes

Russell R. Rhinehart

Warren T. Ford

Dean of Graduate College

ACKNOWLEDGEMENTS

This thesis is dedicated to my parents, Mr. Yupeng Xie and Mrs. Daxi Wang, two people without whom I would never complete my Doctoral work.

I would like to thank my advisor, Dr. Jim Smay and my committee members, Dr. Rinehart, Dr. AJ Johannes, and Dr. Warren Ford for all their help and encouragement. I would also like to thank other people who offered their encouragement and assistance.

Table of Content

List of Figures

List of Tables

NOMENCLATURE

$\dot{\gamma}$	Shear rate
ε	Porosity in the rod
η_{app}	Apparent viscosity
ϕ_{cs}	Chitosan particle weight fraction in colloidal gels
τ	Shear stress or Tortuosity
$\phi_{particle}$	Volume fraction of latex particles
$\phi_{Pluronic}$	Volume fraction of Pluronic polymers
3D	Three dimensional
BSA	Bovine serum albumin
CAD	Computer aided design
CFSE	Carboxy-fluoroscein succinimidyl ester
CLSM	Confocal laser scanning microscope
$C_p(t,r)$	Protein concentration at r and time t
C_s	Protein solubility in chitosan nanoparticles
D/a	Nozzle diameter to particle size ratio
D_e	Effective diffusion coefficient
DMEM	Dulbecco's modified eagle's medium
D_p	Diffusion coefficient of the protein in Pluronic hydrogel
ELISA	Enzyme-linked immunosorbent assay

F	Formation factor
FCS	Fetal calf serum
FDM	Fused deposition modeling
G'	Shear modulus
GFP	Green fluorescent protein
IEP	Isoelectrical point
in vitro	Out of body, in test tube
in vivo	In the body
K	Combined constant
K_r	Restriction factor
M	Mass of protein originally incorporated in scaffold
MFT	minimum film forming temperature
MW	Molecular weight
PCL	Poly(ε-caprolacton)
PCL	Polycaprolactone
PDGF	Platelet-derived growth factor
PHA	Polyhydroxyalkanoate
PLGA	Poly(lactic acid-co-glycolic acid)
PPF	Polypropylene fumarate
QCE6 cell	GFP transfected quail mesodermal cells
r	Radius of the cylinder
R	Radius of scaffold rod
SEM	Scanning electron microscope

SFF	Solid freeform fabrication
SLA	Stereolithography
SLS	Selective laser sintering
TFF	Tangential flow filtration
T_g	Glass transition temperature
T_m	Melting temperature
T_p	Process temperature
TPP	Tripoly-phosphate

Chapter 1 Introduction

1.1 Motivation

A fundamental premise for tissue engineering (TE) is that new functional tissues or organs can be generated by culturing cells *ex vivo* in the appropriate environment to restore tissue or organ function.[1, 2] In most cases, the cells require a three dimensional (3D) porous matrix or scaffold, which provides a framework for cells to attach, proliferate, and differentiate.[3] Commonly held criteria for designing polymer scaffolds are that[4, 5]: the scaffolds should be biocompatible, biodegradable, non-cytotoxic, and. high porous; they should have a customized shape, proper pore size, and suitable mechanical strength; also they should be capable of incorporating biomolecules and subsequent controlled release to provide the chemical cues for tissue formation in right configuration and functions.[6]

Conventional methods of TE scaffold fabrication such as fiber bonding[7], solvent casting/salt leaching[8, 9] suffered a predominant restriction on structural control and they can't make scaffold with complicated and reproducible structures.[4] Solid freeform fabrication (SFF), processes build structures directly from digital geometrical data without a mold, represent attractive tools to prepare 3D scaffolds with customized overall external shape and complex internal structure.[10-13] However, among the expanding number of SFF techniques, relatively few are suitable for incorporation of these biomolecules within the scaffolds because most of them rely on harsh processing conditions, which will denature the highly sensitive biomolecules. For example, biodegradable synthetic polymers such as poly(lactic acid-co-glycolic acid) (PLGA) can be used in existing SFF techniques, but they

have to be melted at elevated temperatures (e.g. fused deposition modeling or selective laser sintering technique) or dissolved in toxic organic solvent (e.g. three dimensional printing technique) in order to be processable. SFF processes using aqueous and room temperature processing conditions would present a benign environment for incorporation of biomolecules, but they are limited to water-soluble polymers or hydrogels that are mechanical weak and lack molecular design flexibility. Clearly, SFF techniques offer superior control of structure compared to bulk processing, but novel SFF technologies have to be developed to overcome the inherent difficulties and limitations in the context of tissue engineering.

In this work, an aqueous, low temperature SFF method for making tissue engineering scaffolds by using polymer colloidal gel as feedstock has been developed. Colloidal gel is a class of materials consisting of a percolating network of attractive colloidal particles. Since the particle network is form by the physical association of the latex particles, when subject to shear above a threshold known as the yield stress, this particle network will be disrupted to exhibit a low viscosity. Upon removal of shear, the particle network will re-establish quickly and return to gel state with high elastic modulus. Thus the unique properties of the colloidal gel, pseudoplastic rheology and rapid structure recovery kinetics, facilitate the material flowing through fine nozzles as a continuous rod and holds its shape to obtain the 3D structures by drawing 2D patterns in successive layers. The composition of the colloidal particles has little effect on the rheological properties such that the ink design allows the exploit of latex particles prepared from mechanically strong but water insoluble synthetic polymers to fulfill the structural requirements of the scaffold. The aqueous suspensions can also contain dual-purpose dissolved biopolymers to render the scaffolds with bioactive

chemistry for cell attachment and proliferation as well as functioning as processing aids for manipulating the rheological properties of the ink. Since the scaffold fabrication process simply rely on the rheology of the colloidal gels and low temperature coalescence of the latex particles, sensitive biomolecules can be incorporated in the interstices of sintered colloidal particle networks and subsequently released without denaturation during tissue culture for regulating cell behaviors.

1.2 Thesis Scope

The main objective of this thesis is to develop an aqueous and low temperature based SFF method for fabricating bioactive scaffolds, which can be used in tissue engineering. This work mainly focuses on two major aspects: 1) to design colloidal gels with appropriate rheological properties based on polymer latex particles and to direct-write biocompatible 3D scaffold with predefined porous structures; 2) to develop strategies for incorporation of proteins into scaffold without activity loss and confer the scaffold with capability of spatial and temporal delivery of proteins. To confirm the validity of the work, comprehensive characterizations of scaffold was performed in this work to examine the biocompatibility of the scaffold and the bioactivity of the released proteins. Finally, the application of this process in fabrication of artificial lymph node was demonstrated.

1.3 Thesis Organization

This thesis is divided up into 5 chapters. Chapter 1 states the motivation of this work, thesis scope, and thesis organization. Chapter 2 is a literature survey pertinent to four inter-disciplinary fields: polymer latex, freeforming of polymers, tissue engineering scaffolds, and drug delivery. Chapter 3 covers the formulation of colloidal gels, rheological analysis

of latex ink, and fabrication 3D scaffolds with various architectures. Chapter 4 presents the methods of incorporation of proteins into the scaffold and characterization their distribution, release behavior and bioactivities. Finally, chapter 5 draws conclusions from the complete work and proposes future directions to improved colloidal gel formulation and cell culture experiments.

Chapter 2 Background

2.1 Polymer Latex

2.1.1 Definition

Colloid refers to system in which one or more of the components have at least one dimension within the nanometer (10^{-9}m) to micrometer (10^{-6}m) range.[14] As a subclass of colloidal materials, polymer latex is an aqueous colloidal suspension of polymer particles, that is to say, the suspension medium is aqueous and the dispersed phase is polymeric in nature.[15]

2.1.2 Particle Interaction

A characteristic feature of colloidal suspensions is the large surface area-to-volume ratio of the particles involved. Interactions between the dispersed particles are evident and play a very important part in determining the physical properties of the system as a whole. The phenomenological and mathematical descriptions of suspension stability and rheology depend on understanding the nature of attraction and repulsion forces between particles.

There are three major inter-particle forces governing colloidal stability: *1) van der Waals forces* are a consequence of the spontaneous fluctuation of the electronic clouds of atoms in one material causing a corresponding fluctuation in neighboring materials, which leads to an attractive force.[16] This long-range force is omnipresent and always attractive between like latex particles and is the predominant driving force for particle aggregation in the suspension systems;[17] *2) electrostatic forces* are resulted from mutual repulsion of particles with a similar surface charge as most latex particles are electrically charged and

with same surface chemistry. The repulsive electrostatic potential energy, V_{elect} decreases exponentially as the distance between particles increases and the magnitude increases with increasing surface charge amount. Additionally, V_{elect} depends on the dielectric properties and ionic strength of the intervening medium. In colloids containing opposite charges, V_{elect} may become attractive and lead to particle aggregation; *3) steric repulsive forces* are genetated between the particles when the particle surfaces in colloids are covered with nonionic material layers (usually polymeric in nature) in order to control the stability of the colloid. When polymer brushes adsorbed on adjacent particles interpenetrate, entropy will decrease and this provides a strong thermodynamic barrier to prevent particle aggregation known as steric hindrance. If the solubility of the adsorbed brush is altered by solvent conditions or a favorable energetic mechanism (e.g. hydrogen bonding) exists, the polymer brush can act to aggregate the particles.

2.1.3 Stability

A suspension in which the particles remain separated from one another for long periods of time is said to be *stable*. There are at least two ways to reduce the tendency for latex particles to aggregate: *1)* e*lectrostatic stabilization*: the particles can acquire the stabilization by electrostatic repulsion between particles, arising from ions that are either adsorbed by or dissolved from the surface of the particles; *2) steric stabilization:* The particles can be sterically stabilized by anchoring a thick layer of nonionic materials, such as hydrophilic polymers, as stabilizer which itself can prevent close approaching. In reality, the two mechanisms of stabilization often occur together whereas probably one is predominant and the other is relatively minor.

In the case that the colloid is electrostatically stabilized, the stabilization mechanism can be explained by DLVO theory.[18] The determinant of colloidal stability is the balance between the *van der Waals* attraction (V_A) and the repulsive potential energy (V_R) resulting from the existence of the electrical double layer (EDL), which is in turn caused by contamination of colloidal particles by electrostatic adsorption of free ions in solution to the their surface.[16, 19, 20] The total interaction potential of latex can be expressed in Equation 2.1.

$$V_T = V_A + V_R = \frac{64 n_0 \pi a k T \gamma^2}{\kappa^2} \exp(-\kappa H) - \frac{A_{121} a}{12 H} \tag{2.1}$$

where V_T is the total energy, n_0 the concentration of counter-ions at infinite distance, a particle radius, k the Boltzmann constant, T the absolute temperature, γ surface potential, $1/\kappa$ the *Debye-hukel* screening length, and H the separation distance between two particles. If a monotonically decreasing energy potential persists up a primary minimum with decrease of inter-particle distances, no energy barrier prevents the system from reaching this minimum and it easily leads to irreversible association or *coagulation*. While if there exist a maximum energy potential prior to the primary minimum and the maximum is sufficiently high, the maximum serves as a barrier to particle coagulation and allows the existence of secondary minimum that may lead to reversible association or *flocculation*. The extent to which the association is reversible between particles depends on the depth of the potential well and on the possible further processes in the aggregate state.

Sterically stabilized latexes may use AB block copolymers, in which the A-block is hydrophilic and B-block hydrophobic, as stabilizers. This molecule sit at a particle/water interface with B-block serving as an anchor and the A-block snaking out into the aqueous

medium. Therefore, this mechanism of stabilization clearly depends upon the free energy of mixing (ΔG_m) between the A-segments of the steric stabilizer and the solvent. If ΔG_m is negative, then there will be favorable mixing such that osmotic pressure mechanism will aggregate the particles. According to Flory-Krigbaum solution theory[21], θ temperature was introduced to specify the conditions under which ΔG_m just goes to zero and beyond which the driving force for stabilization disappears and the system will coagulate.[15] The ΔG_m can be expressed in following equation.

$$\Delta G_m = 2kT\left(\frac{v_s}{v_1}\right)\left(\frac{1}{2}-\chi_1\right)\int \rho_d \rho_d^{'} dv \qquad (2.2)$$

in which v_s is the volume of a chain segment, v_1 the volume of a solvent molecule, χ_1 the Flory-Huggins interaction parameter, and ρ_d and ρ'_d the segment density distribution function of the two inter-penetrating polymer chains, respectively.

2.1.4 Consolidation

The formation of film or bulk from polymer colloids is the most important practical application of latex because of its relevance to the ink and coating industries. Polymer latex consolidation is known to occur in three stages as depicted in Figure 2.1.

Stage I is the water evaporation and particle packing stage. The first significant work on latex drying was performed by Vanderhoff et al.[22] They described drying as a three-stage process and correlated each of the stages with structural changes occurring with film formation. As evaporation of water from latex suspension proceeds, latex particles come closer together and arrange into, preferably, closed packed arrays. The extent of ordering in latex is a function of drying rate, volume fraction of particles, ionic strength, and *etc*.

Stage II is the particle deformation stage during which particles deform under the influence of capillary forces. As soft latex particles dry, they deform from a sphere into a rounded polyhedron and finally to a rhombic dodecahedron structure. Latex particles may coalesce to varying extent, depending on preparation temperature, storage time, and storage temperature.

Stage III is the coalescence stage during which polymer diffusion across particle boundaries, resulting in the formation of a continuous form.[23] To obtain a strong, continuous film or solid bulk, it is necessary that the segments of chain polymer molecules diffuse from one globule to another, thus forming a strong link.[24] This stage of film formation has been found to be dependant on particle size, stabilizer properties, annealing conditions, and diffusion rate of polymer molecules. Increasing of molecular weight (MW) and incompatibility of the latex polymers will generally lowers the inter-diffusion rate.

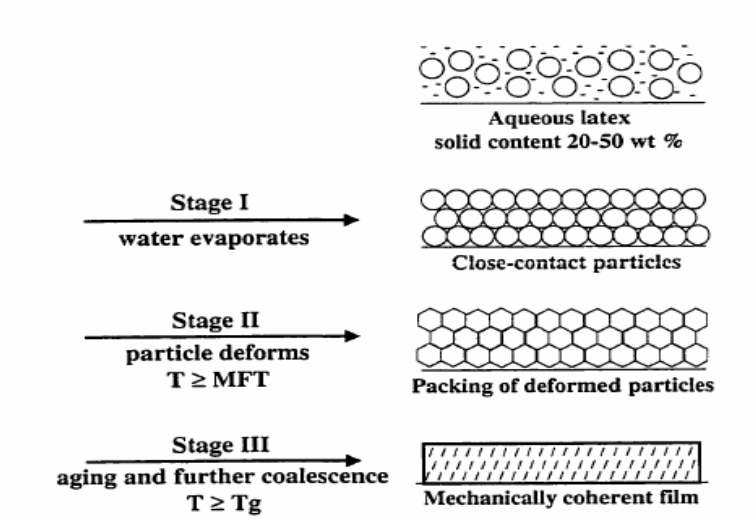

Figure 2.1. Three stages of latex consolidation: stage I water evaporation; stage II particle deformation; and stage III particle coalescence.

2.2 Freeforming of Polymers

2.2.1 Introduction

As opposed to traditional fabrication methods, solid freeform fabrication (SFF) technologies build a designed structure directly from digital geometrical data without a mold. This additive nature offers great promise for producing objects with customized shape, complex internal void, and spatial gradient of material compositions. The basic operations of the various SFF techniques are similar, all employ the same basic five-step procedures[25]: *a)* create a CAD model of the design; *b)* convert the CAD model to stereolithography (STL) format; *c)* slice the STL file into thin cross-sectional layers and generate tool paths; *d)* construct the model one layer atop another; *e)* clean and finish the model.

2.2.2 Major Techniques

Stereolithography was developed by 3D systems, Inc.[26] In the process as shown in Figure 2.2, a He-Cd or Ar-ion laser traces a shape at the surface of a bath of photo-polymerizable monomers (mixture of acrylates or epoxies with a photo-catalyst system), a supporting platform then drops by one layer of thickness and a further layer of monomer is swept across the newly formed surface. The process repeats until the part is completed.

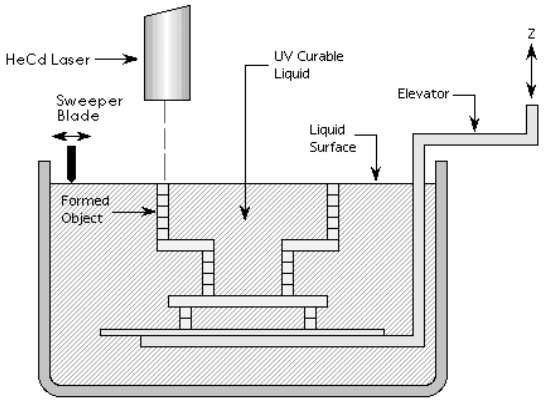

Figure 2.2. Schematic of the stereolithography process (courtesy of techok.com)

SLS (selective laser sintering) uses a CO_2 or YAG laser to sinter powder based materials together layer-by-layer for making a solid model.[27] In the process as illustrated in Figure 2.3, a thin layer of build material is spread across a build platform where the laser traces a 2D cross-section of the part to sinter the material together. The platform then descends a layer thickness and the leveling roller pushes material from the powder cartridge across the build platform, where the next cross-section is sintered to the previous. This continues until the part is completed.

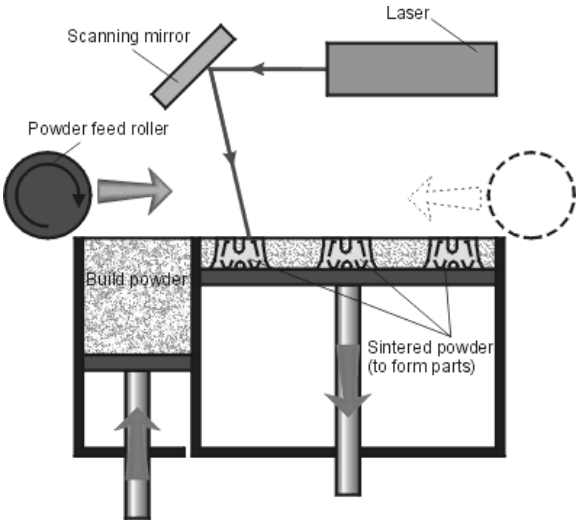

Figure 2.3. Schematic of selective laser sintering process (courtesy of uni.edu)

FDM (fused deposition modeling) is the second most widely used SFF technology after stereolithography.[10] During the process, a plastic filament is unwound from a coil and was supplied to an extrusion nozzle (Figure 2.4). The nozzle is heated to melt the plastic and deposits a thin bead of extruded plastic to form each layer. The plastic hardens immediately after being squirted from the nozzle and bonds to the layer below. The 3D objects can then be constructed layer be layer.

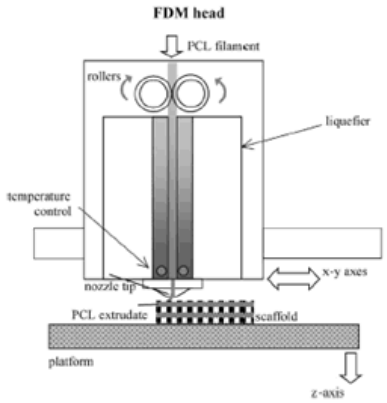

Figure 2.4. Schematic of fused deposition modeling process (courtesy of nus.edu.sg)

3DP (three dimensional printing) was developed at MIT.[12] The process (Figure 2.5) starts by spreading a layer of powders at the top of a fabrication chamber by a roller. The multi-channel jetting head subsequently deposits a liquid adhesive in a 2D pattern onto the layer of the powders which becomes bonded in the areas where the adhesive is deposited. Once a layer is completed, the fabrication piston moves down by the thickness of a layer. The process is repeated until the entire object is formed within the powder bed.

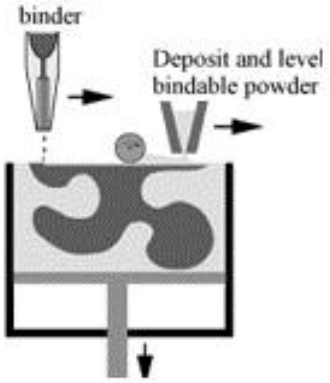

Figure 2.5. Schematic of three dimensional printing process (courtesy of turkcadcam.net)

3-D Plotting (three dimensional plotting) techniques have many different versions but the procedures and equipments are analogous. All of them use a computer-guided robot and a dispenser that is movable in three dimensions (Figure 2.6). The plotting material, being stored in a cartridge, is plotted directly on a plate or into the liquid plotting medium through a syringe mounted on dispenser.[28-30] The material can be solidified either by solvent evaporation or ion crosslinking.

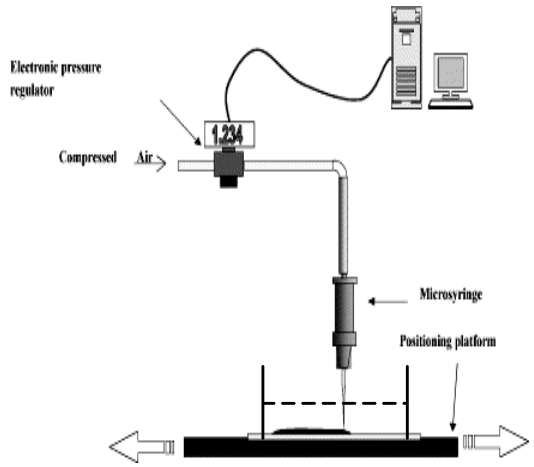

Figure 2.6. Schematic of 3-D plotting process (courtesy of reference [28])

2.2.3 Comparison

The advantages and disadvantages of the SFF techniques for polymer fabrication are listed in Table 2.1. All these techniques share the characteristics of being able to make

object with freeform surface, internal hole, and complex material gradient, which are not achievable by standard forming methods. However to be applied in fabrication of bioactive scaffolds, one must consider other properties if not the processes. Stereolithography is limited to reactive resins, most of which are toxic. Selective laser sintering exposes the supply materials to extreme heating, thus will preclude the use of bioactive molecules in the build process. 3DP techniques are subject to the difficulty of growth factor incorporation, which is important for the subsequent regulation of cellular activity, due to the particle preparation process.

Table 2.1 Capabilities and limitations of various SFF techniques

SFF technique	**Classification**	**Materials**	**Advantage**	**Disadvantage**
Stereolithography	Lithography	Reactive resins	Good mechanical strength	Limited to reactive resins (mostly toxic)
SLS	Lithography	Metals, ceramics, bulk polymers, compounds	High accuracy. Good mechanic Strength. Broad range of bulk materials	Elevated temperature-local high energy input Uncontrolled porosity
FDM	Extrusion	Some thermoplastic polymers/ceramics	Low cost	Elevated temperature Small range of bulk materials. Medium accuracy
3DP	Lithography	Ink + powder of bulk polymers, ceramics	No inherent toxic components, Fast processing	Weak bonding between powder particles
3-D plotting	Extrusion	Swollen polymers (hydrogels), Thermoplastic polymers, reactive resins, ceramics	Broad range of materials, conditions. Incorporation of cells and proteins	Slow processing

2.3 Tissue Engineering Scaffolds

2.3.1 Tissue Engineering

When tissues or organs become diseased or damaged, a physician normally has little recourse but to replace them. Harvesting the patient's tissue from a donor site and transplanting it to a host site has become the "gold standard" for many surgical procedures.[31] However, this therapy has obvious limitations such as donor site scarcity, pathogen transfer, and immune rejection. To address these problems, autogenous tissue transplantation and regeneration based on tissue engineering (TE) technique has emerged as a very promising alternative treatment.[4] With this approach, a biopsy of stem cells obtained from the patient's own tissue is seeded into a temporary 3-D scaffold, which serves as an adhesive substrate and a physical support for implanted cells to proliferate, secret their own extracellular matrices (ECM) and finally form the new tissue or organ. During the process of cell growth, the scaffold gradually degrades and eventually disappears (Figure 2.7).[4]

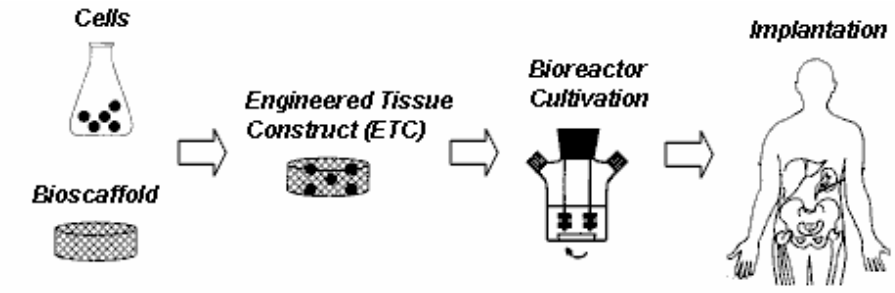

Figure 2.7. Schematic of the tissue engineering approach.

2.3.2 Scaffold Design Criteria

In order to form artificial tissues with right configuration and functions, scaffolds must meet certain design criteria[32-36]: *1) biological aspect:* the scaffold should have a

controllable degradation rate to match the rate of tissue regeneration and cell friendly surface physicochemical features to facilitate cell adhesion, spreading, migration, proliferation *in vitro* and cell recruitment and healing at the tissue-scaffold interface *in vivo*.[37, 38] Neither the scaffold materials nor its degradation products should be toxic or provoke inflammation;[1, 39] *2) structural aspect:* scaffold should have high porosity and pore interconnectivity that allows the unhindered diffusion of nutrients[40] and removal of metabolic waste.[41, 42] Scaffold should have high internal surface area to accommodate the large numbers of cells and controllable pore size to fit various tissue microenvironment; *3) mechanical aspect:* scaffolds should have sufficient mechanical strength during *in vitro* cell culturing to manage any *in vivo* stresses and physiological loadings, especially for regenerating load-bearing tissues (e.g., cartilage, bone).[42, 43] The degradation behavior of the scaffold should be designed so that it retains sufficient structural integrity until the newly grown tissue has replaced the supporting function of the scaffold.[42]

2.3.3 Scaffold Materials

The most common biomaterials used for tissue scaffolds fall into two major categories: *synthetic polymers*, and *natural polymers*. *1) Synthetic polymers* have the distinct advantages that their mechanical, chemical, and biodegradation properties can be engineered by molecular design to fit a particular need.[44] Poly(lactic acid), poly(glycolic acid), and their copolymers PLGA are the most widely used synthetic biodegradable polymers available[45, 46] because of their controllable degradation rate and highly regulated metabolic removal mechanism of their degraded monomeric components.[47, 48] Due to these properties, PLGA materials have been used extensively to fabricate scaffolds for engineering musculoskeletal tissue, including scaffolds for bone,[49-51] cartilage,[52-55] and

meniscus.[56] 2) *Natural polymers:* naturally occurring polymers such as collagen and glycosaminoglycan (GAG) based materials are the most widely used natural polymers in tissue engineering[57, 58] The prevalence of collagen in the majority of human tissue underlies its ability to support the growth and function of a wide variety of cell types. In particular, GAG has been shown to regulate cell functions and play an important role in tissue development and repair.[59] However, natural polymers have major limitations, such as poor mechanical property control ability and potential immunogenic properties.

2.3.4 Scaffold Fabrication

The scaffold fabrication processes are also subject to certain requirements. First, the processing conditions should not adversely affect chemical properties and biocompatibility of the scaffold nor cause any degradation in its mechanical properties. The processing route should lead to spatially and anatomically accurate 3-D scaffolds structures. Also different scaffold batches are supposed to exhibit minimal variations in physical forms and properties when produced from the same set of processing parameters. In addition, the technique should be able to produce scaffolds that fit the intended spaces at the implant site with controlled pore morphologies, pore distribution and interconnectivity designed for each tissue engineering application.

Conventional techniques of scaffold fabrication include fiber bonding[60, 61], phase separation[62, 63], solvent casting/particulate leaching[35, 64-66], membrane lamination[67], melt molding [68], gas foaming/high pressure processing[69, 70], hydrocarbon templating[71], freeze drying [72, 73] and combinations of these techniques (e.g., gas foaming and particulate leaching[74]). Although these methods have been applied to engineer a variety of tissues with varying success, they are limited by numerous drawbacks which restrict their scope of

applications, such as extensive use of toxic organic solvents[73], residual porogen,[75] and highly inconsistent macro- and micro- structures (pore sizes, pore morphologies, porosities and internal surface areas).

2.4 Controlled Release

2.4.1 Introduction

A controlled release system is a combination of active agent and excipient, commonly a polymeric material, designed to allow delivery of the agent to the target at a controlled rate over a specified period of time.[76, 77] According to the mechanism used to control the drug release, the design of controlled release devices is mainly based on one of these categories: *1)* diffusion controlled system, *2)* bioerodible controlled system, and *3)* swelling controlled system.[78-84]

2.4.2 Diffusion Controlled System

In terms of diffusion controlled system, polymeric materials are designed either in the form of the carrier materials or the permeable membranes to form two basic types of diffusion controlled systems[85]: *matrix a*nd *reservoir* devices. A reservoir device (Figure 2.8(a)) is the simplest diffusion-controlled system consisting of an inert diffusion barrier membrane enclosing the active agent to be released. The drug release rate is determined by choice of membrane material and partition coefficient of the drug to be released. In a *matrix* device (Figure 2.8(b)), the active agent is uniformly dispersed, either molecularly or as solid drug particles, throughout an inert polymeric matrix. The drug release can be modified by varying of drug loading, nature of carrier material (polymer) and additives, and device geometry.[81]

Figure 2.8. Schematic diagram of the diffusion controlled system: (a) matrix system and (b) reservoir system

The release rate in diffusion controlled system is essentially governed by the Fick's diffusion law. The principal advantage of reservoir system is the ease they can be designed to achieve zero order release profile, the ideal kinetics from a pharmaceutical standpoint. The release rate of membrane controlled reservoir is determined by the following equation:

$$\frac{dM_t}{dt} = -\frac{DKA}{\delta}(C_2 - C_1) \tag{2.3}$$

where D is the diffusion coefficient, δ the membrane thickness, M_t the amount of drug release at time t, K the partition coefficient, A the surface area, and C_2 and C_1 are the drug concentration inside and outside of the membrane, respectively. To maintain a constant flux, the drug can be loaded to a level far above the solubility of the drug to keep the drug concentration gradient constant. In matrix systems, the drug release kinetics is calculated as in Equation 2.4. for drug loaded spherical particles under perfect sink condition.[86]

$$\frac{M_t}{M_\infty} = 1 - \frac{6}{\pi^2}\sum_{n=1}^{\infty}\frac{1}{n^2}\cdot\exp(-\frac{D\cdot n^2\cdot\pi^2\cdot t}{R_s^2}) \tag{2.4}$$

where M_∞ is the amount of drug release at infinite time and R_s denotes the radius of the particle. Generally, the release rate is proportional to $t^{1/2}$ in short time and exhibits exponential decay for long time.[87]

2.4.3 Bioerodible Controlled System

In these systems, the drug is distributed throughout a polymer in the same way as in matrix systems. The difference, however, relates to the fact that drug release is due to the erosion of the polymer phase instead of diffusion. The rationale for using biodegradable or bioerodible systems is that the devices are eventually adsorbed by the body or environment and do not require removal after administration.[88, 89] The mechanism(s) of polymer degradation can be either surface degradation, bulk degradation, or the combination of both (Figure 2.9).

Figure 2.9. Schematic diagram of the bioerodible controlled system: (a) surface erosion system and (b) bulk erosion system.

The release kinetics of bioerodible controlled release device depends on the biodegradation rate of the polymer and is generally expressed as follows.[82]

$$\frac{dM_t}{dt} = K_e A_e \tag{2.5}$$

where K_e is the reaction or dissolution rate, A_e is the instant surface area. For various geometries, the solution to this expression is:[82]

$$\frac{M_t}{M_\infty} = 1 - \left[1 - \frac{k_e t}{C_0 \frac{\delta}{2}}\right]^n$$

Geometry	δ	n
slab	thickness	1
cylinder	diameter	2
sphere	Diameter	3

(2.6)

Thus, to obtain zero order release, it is necessary to utilize a geometry where the surface area does not change as a function of time, a slab is such a shape, on the other hand, sphere and cylinder would display decreasing rates with time because their surface area would diminish.

2.4.4 Swelling Controlled System

In swelling controlled systems, the bioactive agent is originally dissolved or dispersed within a glassy polymer matrix and there is no drug diffusion. As the environment fluid penetrate the matrix, the polymer swells into a rubbery state and it allows the incorporated drug to diffuse outward.[90] The dimensionless diffusion Deborah number D_e defined as the ratio of the characteristic stress relaxation time of the polymer swelling agent system, λ to the characteristic time for the diffusion of the dissolution medium θ, characterize the region of observation of Fickian or non-Fickian (anomalous) diffusion.[91, 92] Fickian diffusion is observed for $De >> 1$ or for $De << 1$, non-Fickian diffusion behavior occurs when D_e of order one. Drug release from a thin slab, under countercurrent diffusion of a swelling agent in a glassy polymer may be expressed by equation.

$$\frac{M_t}{M_\infty} = kt^n \tag{2.7}$$

Where k is a empirical factor. Fickian diffusion occurs when $n = 0.5$, while Non-Fickan diffusion is characterized by $n > 0.5$.

Chapter 3 Tissue Engineering Scaffold

3.1 Introduction

The goal of tissue engineering is to regenerate bodily tissues by seeding cells onto three-dimensional (3D) porous matrices, know as scaffolds, which direct the cell growth and tissue remodeling.[2, 93, 94] The common practice of seeding cells on two dimensional (2D) substrates often leads to distorted metabolism and gene expression pattern and cell morphology owing to altered extracellular context.[95] Alternatively, culturing cells in 3D scaffolds results in a microenvironment more closely resembling that found *in vivo*[96] such that the seeded cells respond to mechanical and biological cues from the all 3D locations that promote cell adhesion, proliferation and differentiation. Suitable tissue scaffolds are subject to certain design criteria, e.g. scaffolds should have features such as interconnected pore structure, cell friendly surface chemistry and incorporated vital growth factors that are released to encourage successful tissue growth.[32-36, 43]

During the past decades, a variety of techniques have evolved to build 3D structures for tissue scaffolds.[10-13] Conventional techniques of scaffold fabrication, such as salt leaching, by using simple porogens have had only limited success in fabricating scaffolds with complex microstructures.[97] Solid freeform fabrication (SFF) technologies have shown varying success in fabricating scaffolds with designer internal and external microstructures, with better control over localized pore morphologies, porosities, and material composition to suit the requirements of multiple cell types arranged in hierarchical structures.[1, 98, 99] However, most SFF processes require harsh processing conditions like

elevated temperature, toxic solvents, or intense local radiation.[100] Such settings would denature highly sensitive biomolecules (e.g. growth factors); hence precluding their use to modulate cell growth and restricting their scope of applications. The benefits of including growth factors, which have been observed in several solvent-free, aqueous processes, have been limited to crosslinkable hydrogels, which may be physically weak and lack molecular design flexibility.[101]

Here, an aqueous, low temperature based SFF technique for scaffold fabrication was developed. The SFF process consists of formulating colloidal gel with polymer latex particles to be used as inks in a 3D direct write process. The colloidal gel has rheological properties that allow for it to be extruded as a rod with circular cross section. The extrusion nozzle is moved relative to a substrate to draw two dimensional patterns and 3D structures result when the 2D patterns are drawn in successive layers. The ink design allows the use of latex particles prepared from mechanically strong but water insoluble synthetic polymers as the colloid phase. Unique to selective laser sintering (SLS) or fused deposition modeling (FDM) techniques that require the feedstock to be processed at a temperature beyond its melting temperature (T_m), the colloidal gel based technique only demand the processing temperature comparable to or higher than the glass transition temperature (T_g) of the latex polymers, which is far lower than the corresponding T_m. In addition, this process is further facilitated by the capillary forces generated in water evaporation that drive particle densification to increase structure integrity. Upon drying of the ink, the polymer particles consolidate under biologically benign conditions (aqueous, < 37 ^{o}C) to evolve mechanical strength. Consequently, labile biomolecules, solitarily or microencapsulated, may be incorporated in the ink design by co-dispersion with latex particles to be released upon

seeding of the scaffold. The aqueous suspensions also contain dual-purpose dissolved biopolymers to impart the scaffolds with bioactive chemistry for cell attachment and proliferation as well as functioning as processing aids for manipulating the rheological properties of the ink. For successful printing in the SFF process, two critical behaviors are required of the ink: *1)* it must flow readily through a small nozzle; *2)* it must set rapidly to retain its shape.

As a model system, non-degradable polyacrylate was chosen in this work for latex particles because it has a long history of being applied in biomedical fields.[102, 103] Also its resistance to degradation during scaffold fabrication and rheological characterization ensures latex compositional and structural stability during the entire deposition and rheological characterization. Nevertheless, the process described in this paper can be easily transferred to other synthetic biodegradable polymer such as PLGA and PCL, which will be discussed later. The inks described here consist of latex particles and poly(ethylene oxide)-poly(propylene oxide) (Pluronic) block copolymers in aqueous solution. Ink rheological properties were characterized as a function of particle volume fraction and binder concentration. In addition, cell culture and cell viability testing were performed to check cytotoxicity.

3.2 Materials and Methods

3.2.1 Material System

Acrylic polymer latex (Elotex Titan 8100, National Starch & Chemical, Bridgewater, NJ, USA) was generously donated. As described by the manufacture, the latex has a glass transition temperature (T_g) of 10 °C and minimum film forming temperature (MFT) of 0

°C. The latex is in the form of a granular powder and can be easily redispersed in water due to an adsorbed poly(vinyl alcohol) stabilizer. The average particle size of the latex samples is about 0.5 μm. Acrylic polymer was chosen because it has a long history of being applied in biomedical fields.[102, 103] Also its resistance to degradation during scaffold fabrication and rheological characterization ensures latex compositional and structural stability during the entire deposition and rheological characterization. Nevertheless, the process described in this paper can be easily transferred to other synthetic biodegradable polymer such as PLGA and PCL. Chitosans (Sigma-Aldrich, St Louis, MO, USA) of medium viscosity (200-800 cP) and low viscosity (20-200 cP) were purified before use by passing the 1% chitosan acetic acid solution through a paper filter, precipitating with NaOH solution, washing twice, and drying in a freeze dryer. The viscosity of chitosan solutions was measured in a capillary viscometer and molecular weight (MW) of the chitosan was calculated according to method previously described.[104] Tripolyphosphate (TPP), bovine serum albumin (BSA) and Pluronic F127 (cell culture tested) were all purchased from Sigma-Aldrich and used as received.

3.2.2 Formulation of Colloidal Gels

Prior to material formulation, the latex particles were dispersed in a large quantity of distilled water for purification. Next, the suspended latex particles were centrifuged (20000×g for 30 min), decanted, redispersed in distilled water and treated with 2~5 g silica gel (Davidsil grade 923, Sigma-Aldrich, St. Louis, MO, USA). After each treatment, the silica gel was separated by use of a stainless steel sieve (pore size 50μm). The centrifugation–redispersion-silica treatment cycles were repeated at least five times.

Finally, the latex was cleaned by dia-filtration with distilled water using a tangential flow filtration (TFF) system (Labscale TFF, Millipore, Billerica, MA, USA) and freeze dried.

The calculated amount of Pluronic F127 was first dissolved in distilled water at temperature of 4 ^{o}C. Next, an appropriate volume fraction (0.47 ~ 0.62) of latex particles was added to the solution and a stable suspension was formed. The suspension was vigorously homogenized for 5 min using a homogenizer followed by processing with a three-roll mill for 5 minutes. The suspension was brought to room temperature and the final colloidal gel was formed due to the thermogelling behavior of the Pluronic binder at ambient temperature. In this work, the volume fraction of latex particle in the total material is designated as $\phi_{particle}$ while the volume fraction of Pluronic F127 (assume density = 1.0 g/ml) in the total material is designated as $\phi_{Pluronic}$. The volume fraction of Pluronic F127 in the liquid phase is designated as $\phi'_{Pluronic}$.

3.2.3 Rheological Characterization

The rheological properties of colloidal gels were characterized using a controlled stress rheometer (Bohlin C-VOR, Malvern Instruments, Southborough, MA, USA) fitted with a C-8 cup-and-bob geometry. The apparent viscosity (η_{app}) was measured in stress viscometry mode, which has a stress range of 0.01 to 500 Pa with a lower shear rate limit of 0.05 s^{-1}. Shear rate ($\dot{\gamma}$) data were acquired as a function of shear stress (τ) in an ascending series of discrete steps with a 1 min equilibration time at each stress. The elastic shear modulus (G') was measured in oscillatory mode, which has a stress range of 0.01 to 500 Pa, a strain sensitivity of about 10^{-4}. G' was measured by performing a stress sweep at a frequency of 1 Hz. The stress sweep was repeated several times after observing a

quiescent equilibration time of ~1 h between measurements. All measurements are performed at 25 ºC using a specially designed solvent trap filled with deionized water to minimize evaporation.

3.2.4 Robotic Deposition of Scaffold

In this study, a specially designed gantry robotic deposition apparatus (Aerotech Inc, Pittsburgh, PA, USA) was used to control the position of the deposition nozzle for scaffolds fabrication (Figure 3.1). Three axes of motion control (X, Y, and Z-axis) were provided by the gantry system and a material delivery assembly comprised of a syringe as reservoir was affixed on the z-axis motion stage. The z-axis motion stage assembly was mounted on a moving X-Y gantry to enable controlled motion of the mounted syringe in three dimensions. A fourth linear actuator (U-axis) served to depress the plunger of the syringe at a fixed speed such that the volumetric flow rate could be precisely controlled. The material housed in the syringe was deposited through a cylindrical nozzle (diameter = 150 μm) such that the extruded filament is bent immediately after exiting the nozzle to lie parallel to the x-y plane. Toolpath design and motion control were accomplished with custom software designed by the investigators.

Polymer scaffolds were fabricated by directly dispensing the colloidal gel material onto a polypropylene plastic film using the robotic deposition device. The 3D meshes were assembled by depositing arrays of lines one atop another. The cuboid scaffolds with tetragonal symmetry were assembled by stacking layers with alternating aligned linear rods along x or y-axis such that their orientation was orthogonal to the previous layer. The rod spacing for the layers was varied from 300 to 1200 μm and the rod diameter was held

constant at 150 μm. The resulting theoretical volume fractions of rods in the scaffold varied from 0.58 to 0.86. The cylindrical scaffolds with radial symmetry were constructed with sequential deposition of layers having alternating patterns of concentric rings and a polar array of radially oriented rods. 150 μm nozzles and deposition speed of 5 mm/s were used in the assembly of these structures. The layer spacing was fixed at 95% of the nozzle diameter.

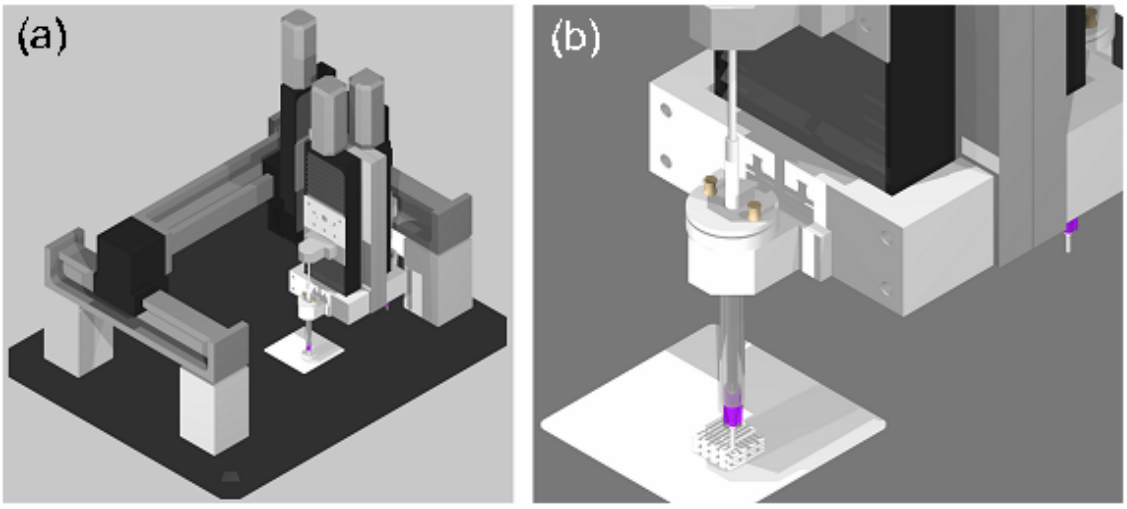

Figure 3.1. 3-D drawings of (a) the robotic deposition apparatus and (b) the syringe holder on the fourth actuator.

Immediately after deposition, the wet scaffolds were dried in an incubator at a constant temperature of 37 ^{o}C for at least 1 hour. The drying behavior was observed by weighing the scaffold at various times during the drying. To arrest the further particle deformation and coalescence, the dried scaffolds were stored in a – 30 ^{o}C freezer. The dried scaffolds were cut with an ultra-short pulse laser through the intersections between rods to reveal the internal structure. The scaffolds were observed under the scanning electron microscope (SEM) to assess the morphology.

3.2.5 Cell Culture

Green fluorescent protein (GFP) transfected quail mesodermal cells (QCE6) were generously provided by Dr. Carol A. Eisenberg (Medical University of South Carolina, Charleston, SC) [105]. The inherent GFP fluorescence of the cells was utilized as an indicator of cell viability (fluorescent = living, non-fluorescent = dead). In this study, the QCE6 cells were seeded onto the fabricated scaffolds and kept in culture for 14 days to determine cytotoxicity of the scaffold material on cultured cells. First QCE6 cells were detached from the flask by applying 0.25% Trypsin/EDTA and counted with a hemocytometer. The cell suspensions were centrifuged and cell pellets were re-suspended in the media to a cell density of 1 million per ml. Cuboid scaffolds (L×W×H = 1.2 mm× 1.2mm ×0.9mm, rod diameter = 150 μm, rod spacing= 300 μm) were immersed in 70% ethanol for 5 min, subsequently washed three times with water and then coated with 1% alginate prior cell seeding. Aliquots of 30 μl cell suspensions were pumped into the scaffolds with a syringe pump (Harvard apparatus, Holliston, MA, USA) at a rate of approximately 3 ml/hour in the complete SAGM media. The cells were kept at 37 ^{o}C by a microscope stage warmer, and seeding of the scaffold was monitored by intermittent epi-fluorescent microscopy. Cultures were maintained at 37^{o}C with 5% CO_2 in a humidified chamber for a two week period. At the termination of the experiment, the formed tissue constructs were examined by a confocal laser scanning microscope (CLSM, Leica SP2, Bannockburn, IL) set to detect GFP. The fluorescence image of tissue construct was obtained by optically scanning in the x-y planes (parallel to the substrate) with 26 scan averaging from top of the scaffold. The total z scanning depth is 250 μm and each slice is 10 μm in thickness.

3.3 Results and Discussion

3.3.1 Rheology of Colloidal Gels

The apparent viscosity (η_{app}) as a function of shear rate ($\dot{\gamma}$) for concentrated latex gels ($\phi_{particle}$ = 0.57) containing various amount of Pluronic F127 is plotted in Figure 3.2(a) and the elastic modulii (G') of the colloidal gels are plotted as a function of stress amplitude (τ) in Figure 3.2(b). When the Pluronic volume fraction[†] ($\phi_{Pluronic}$) was 0.05, the latex suspensions displayed only weak shear thinning and a negligible yield stress as shown in Figure 2.2(a). With the increase of Pluronic addition from 0.05 to 0.06, η_{app} of the latex suspension was boosted almost 10 fold at low shear rate and its rheological behavior became significantly shear thinning. Beyond this Pluronic concentration, the colloidal gels strengthened and exhibited pseudoplastic behavior with a yield stress. This shear thinning with yield stress rheology can be described by the Hershel-Bulkley model given by

$$\tau = \tau_y + K\dot{\gamma}^n \tag{3.1}$$

where τ_y is the yield stress, n is the power law index, and K is the consistency index. In Figure 2.2(b), G' displayed a well-defined plateau (G'_{eq}) in the linear viscoelastic region as the stress amplitude was increased. When the stress amplitude reached the yield stress, G' rapidly decreased. The yield stress was considered to occur when $G' = 0.9G'_{eq}$. [106] As illustrated in Figure 2.2, the addition of increasing amounts of Pluronic polymer results in a gradual increase in both the η_{app} and G' for the gelled latex suspension. Interestingly, η_{app} of the latex gels reach a maximum at about $\phi_{Pluronic}$ = 0.08 and begin to decrease with

[†] $\phi_{Pluronic}$ is the with respect to the total volume of the suspension, the volume fraction in the liquid phase is $\phi'_{\text{Pluronics}} = \phi_{Pluronic}(1-\phi_{particle})^{-1}$

further increase of $\phi_{Pluronic}$. This behavior suggests that the Pluronic is adsorbed to the latex particle surface and forming a hydrogen bonded gel network, however at high concentration of Pluronic, particle poor regions of gel may exist that weaken the overall structure.

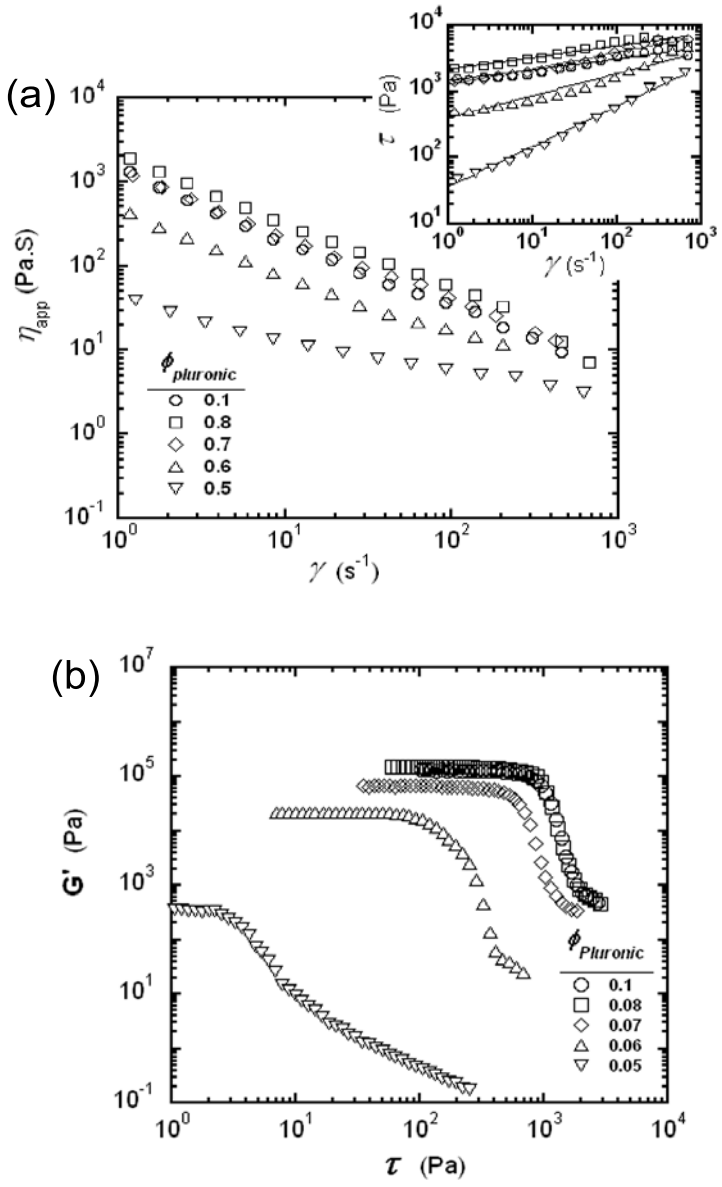

Figure 3.2. Rheological behavior of latex gels with fixed $\phi_{particle}$ = 0.57 illustrating (a) apparent viscosity (η_{app}) and (b) shear modulus (G') as a function of varying $\phi_{Pluronic}$ and shear rate ($\dot{\gamma}$) or shear stress amplitude (τ), respectively. The inset demonstrates the fit of the Hershel-Bulkley model for shear stress (τ) as a function of $\dot{\gamma}$.

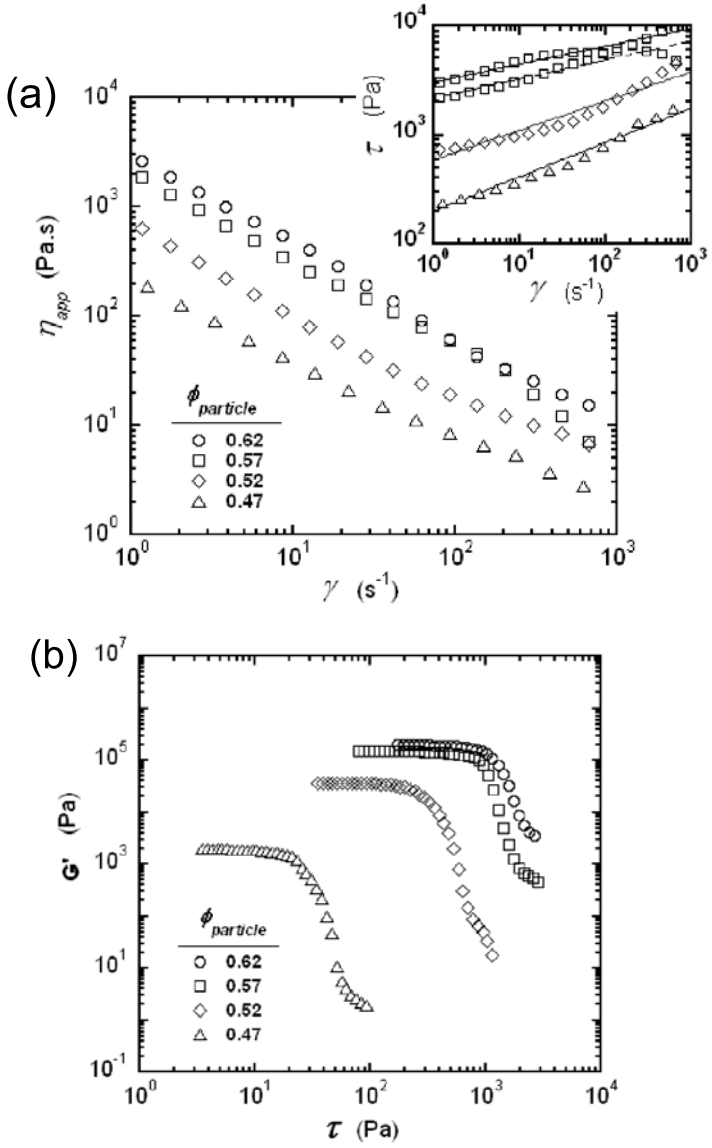

Figure 3.3. Rheological behavior of latex gels with $\phi_{Pluronic}$ = 0.08 illustrating (a) apparent viscosity (η_{app}) and (b) shear modulus (G') as a function of varying $\phi_{particle}$ and shear rate ($\dot{\gamma}$) or shear stress amplitude (τ), respectively. The inset demonstrates the fit of the Hershel-Bulkley model for shear stress (τ) as a function of $\dot{\gamma}$.

The effect of latex particle volume fraction ($\phi_{particle}$) on suspension rheology and viscoelastic properties are shown in Figure 3.3(a) and Figure 3.3(b), respectively. For each suspension, $\phi_{Pluronic}$ = 0.08 ($\phi'_{Pluronic}$ = 0.151~ 0.211). At this Pluronic concentration, all latex suspensions measured exhibited shear-thinning with yield stress rheology, suggesting

the validity of the Hershel-Bulkley model within the $\phi_{particle}$ range. As expected, η_{app} and G' increase with increasing of $\phi_{particle}$ for the colloidal gels. At $\phi_{particle}$ = 0.50, the yield stress of the colloidal gel is 13.8 Pa and increases more than 10 fold to 164 Pa when $\phi_{particle}$ = 0.55. With $\phi_{particle}$ = 0.62, the system approaches the maximum solids loading and processing become extremely difficult.

With the initial addition of Pluronic into acrylic latex suspension, the tri-block copolymer is expected to adsorb such that the hydrophobic PPO section in the middle anchors on the particle surface whereas the solvated PEO blocks extend out into the solution as tails and loops[107] as shown in Figure 3.4. Pluronic forms a hydrogel at room temperature when the concentration in solution exceeds ~20%. The gels shown here have a maximum concentration of Pluronic in the liquid phase of 23%, but significant gelation below this concentration suggests that PEO strands extending from neighboring particles can participate in a gel network at lower concentrations.[108] The particles act to further strengthen the colloidal gel structure. Beyond the minimum gel point, additional linkages form between particle cluster with the further addition of Pluronic resulting in the observed increase of η_{app} and G'. This gelation behavior can also be expected to happen as the particle volume fraction increase over a threshold value as it has the similar effect to encourage the entanglement and association of Pluronic chains.

The colloidal gels initiated by physical association of the Pluronic coated particles are not strong enough to keep the network intact when subject to high shear conditions such as deposition. In this case, the colloidal particulate network becomes temporarily disrupted to exhibit a shear thinning rheology. [109-113] Upon returning to a quiescent state, the network is re-established rapidly and the material returns to the gel state.[106, 114] The ability to break

down and re-build their structure makes gel-based materials well suited to fulfill the requirements of flow through a deposition nozzle with low viscosity and to rapidly "set" to maintain the shape of the deposited filament even as it spans gaps in the underlying layers. Thus colloidal gels possess viscoelastic behavior that makes them ideally suited for assembling such structures. [106, 109-112, 115-122]

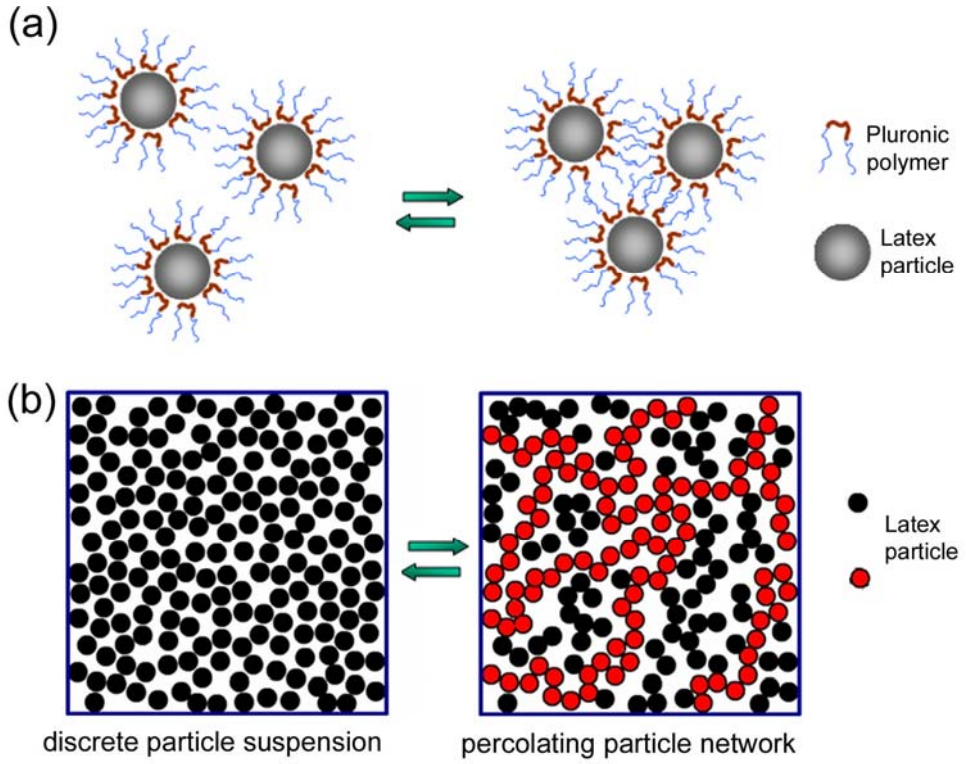

Figure 3.4. (a) Schematic of the conjectural configuration of suspended latex particles with Pluronic polymer chains adsorbed on the surface with middle PPO section anchors on the particle surface whereas the PEO blocks extend out into the solution. (b) Schematic of the reversible particle networks existed in the colloidal gel. The colloidal gel has a unique feature that it can undergo a reversible transformation between the discrete particle suspension when under high shear (left column) and percolating network structure once return in quiescent state (right column)

3.3.2 Scaffold Fabrication

Scaffolds with periodic lattice structure of tetragonal and cylindrical symmetry, shown in Figure 3.5, were assembled from colloidal gel based materials. The cuboid scaffold in Figure 3.5(a) is a lattice of rods stacked with simple tetragonal symmetry, where the rod spacing within each layer resulted in a planar filling fraction of 0.50. As can be seen in Figure 3.5(b) and (c), the scaffold rods maintained a circular cross section and spanned the gaps in underlying layers with minimal deflection. The cylindrical scaffolds in Figure 3.5(d), (e), and (f) have a radial symmetry built by stacking layers of arrays of radial lines between layers of concentric rings. The pore size and volume fraction in these structures decreases from the outer to inner radius.

The diverse nature of tissue architectures requires controlled variation of the microenvironment for cell proliferation and differentiation. Favorable pore sizes and pore structure along with strut size between pores are critical factors. The nominal feature size of the extruded material filament is in the range of 100~200 μm but 50 μm has been successfully accomplished. Filaments in this size range are regarded as near optimal for culturing a variety of mammalian cells.[12, 123] With a fixed deposition nozzle size, the robotic deposition process used here may assemble scaffolds with variation in pore sizes and volume fraction porosity as shown in Figure 2.6. A larger spacing between adjacent lines within a layer result in an increased pore size and volume fraction. Scaffold (1) contains the smallest lattice spacing and has a pore volume fraction of 0.23. The lattice spacing was increased such that the porosity becomes 0.86 in sample (10).

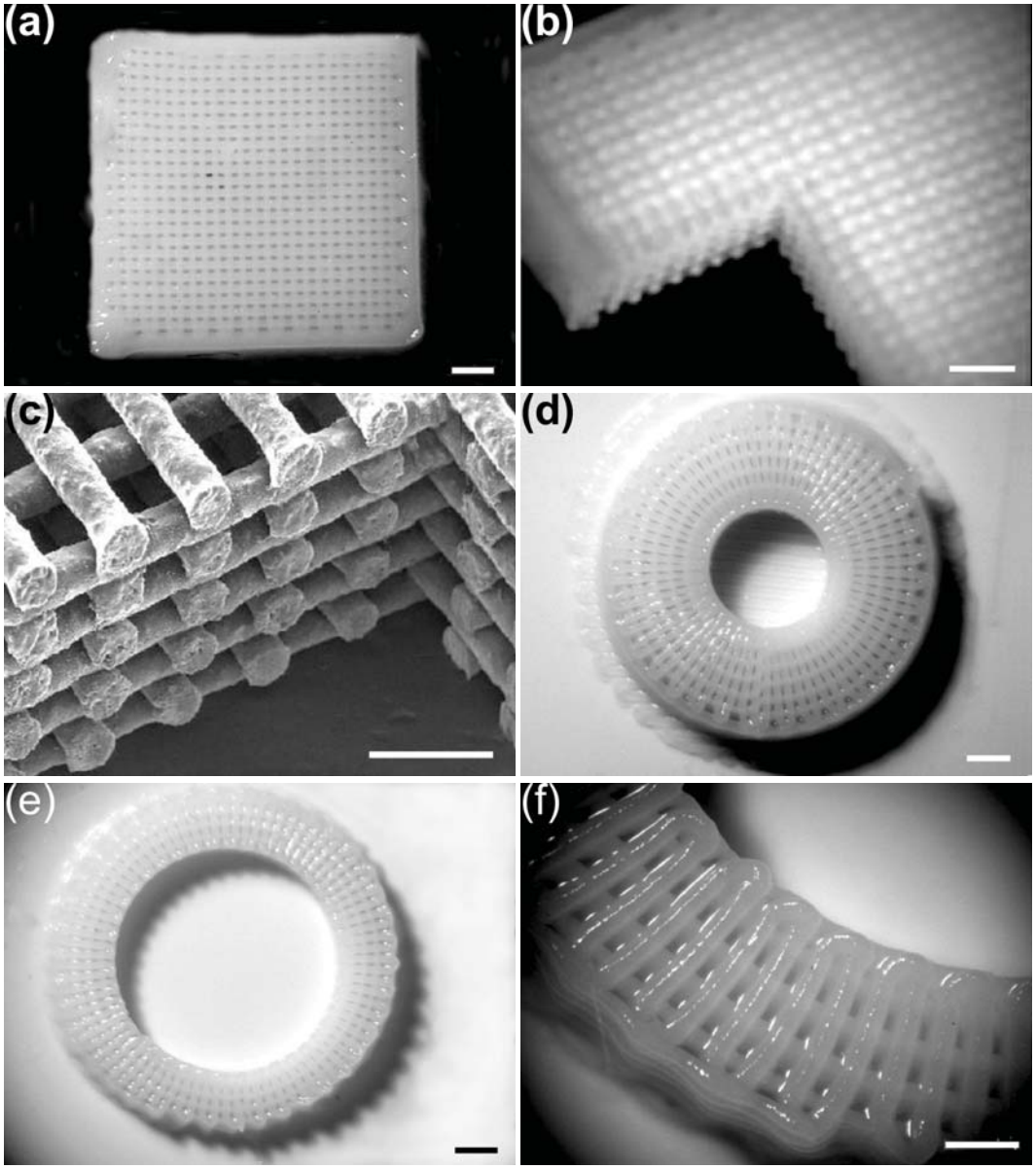

Figure 3.5. Scaffolds formed by deposition of colloidal gel material. (a) cuboid scaffold with a simple tetragonal symmetry; (b,c) internal structure of cuboid lattices reveal the high integrity interfaces formed between layers and circular cross section of lattice rods; (d,e,f) cylindrical symmetry scaffolds. Scale bars (a,b,d,e) 1 mm (c, f) 100 μm

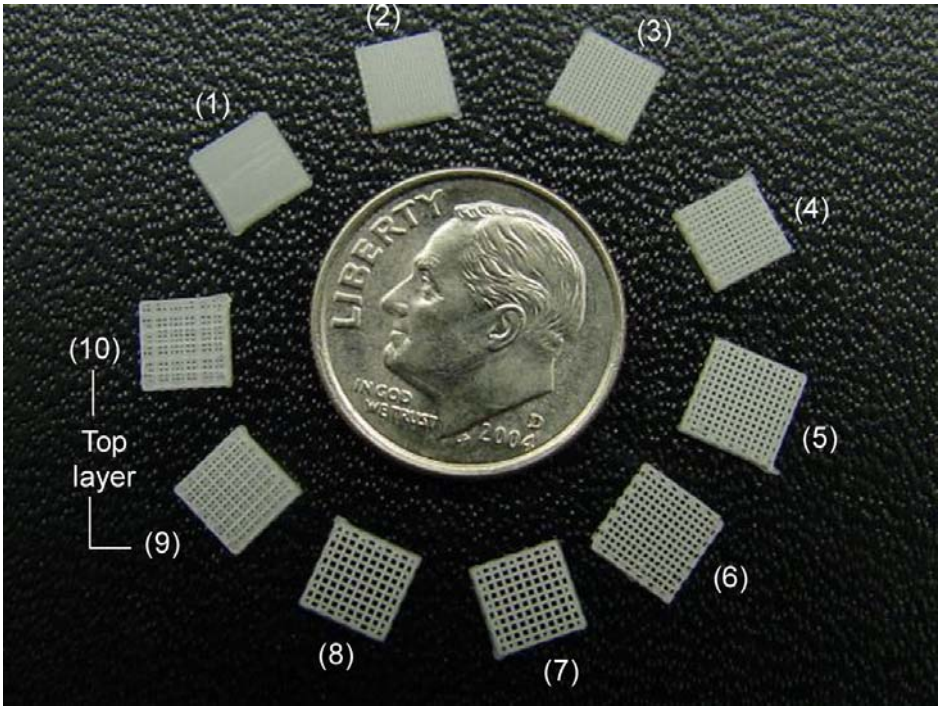

Figure 3.6. Microscopic images of stiffened scaffold with varying rod spacing, resulting in various porosity ranging from 0.23 to 0.86. All the rods in the scaffolds have the same diameter of 150 μm.

3.3.3 Cell Culture

To assess the suitability of the polyacrylate produced here for tissue engineering applications, GFP transfected quail mesodermal stem cell line QCE6 was seeded into the tissue scaffold. Within 5 hours of seeding, the cells began to attach onto the scaffold surface and express their own extracellular matrix. During the first week, cells were seen to actively grow along the rod and bridge across the pore structure. The cell clusters were seen to occupy the interconnected pore space of the scaffolds. By day 10, cells were seen throughout the entire scaffold in three dimensions. Before the termination of the culture, most of the cells appeared healthy and kept the 3D spherical phenotype.

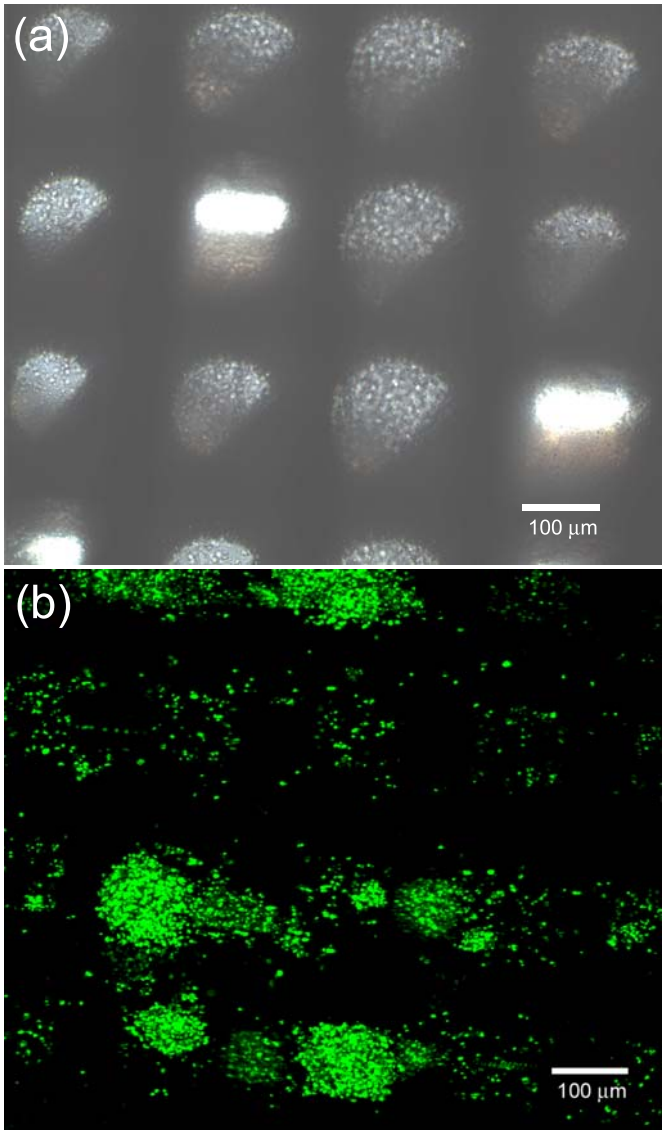

Figure 3.7. GFP transfected Quail mesenchymal QEC6 cells cultured on tissue scaffold. (a) GFP positive cell aggregates are readily observed within the openings of the lattice network. (b) CSLM image illustrating expression level of QEC6 cells. White arrows indicate scaffold rods.

To assess the cytotoxicity of the scaffold materials, GFP expression of the QCE6 cell in scaffold was evaluated by analyzing the fluorescence images acquired by confocal laser scanning microscopy as illustrated in Figure 2.7. Although the mean fluorescence intensity decreased over time, the GFP expression was still significant after 10 days in

culture. The result demonstrates the ability to culture GFP positive cells on the scaffold material while maintaining viability of the cells over the 14-day period, suggesting minimal cytotoxicity of the scaffold material to quail stem cell line. Previous experiment on cell culture by encapsulating HepG2 cells with Pluronic F127 resulted an unsuccessful result. No cell growth was found in the Pluronic gels and most of the cells have died after 6 days. This failure was likely due to poor oxygen and nutrient diffusion within the gels.[124]

3.3.4 Implication of the Material Design

The utilization of polymer colloidal gels for robotic deposition of scaffolds imposes no intrinsic limits on particle properties, provided a gel with the desired rheological properties may be formulated. The deposition feature size, however, is primarily dependent on latex particle size. From previous experimental observation, the requirements of the nozzle diameter to particle size ratio (D/a) > 300 based on the average particle size or D/a > 40 based on the largest particles are normally applied.[125] Therefore, nanometer sized colloidal particles may be used to achieve higher D/a and, hence, smaller feature size.[126]

The mechanical strength of the deposited scaffolds evolves in a three step process. First, upon exiting the deposition nozzle, the colloidal gel has enough strength to maintain its shape, but cannot be easily handled. Second, as water evaporation progresses, the capillary forces developed at latex surface drives particle compression and densification, resulting in a stronger scaffold. However, the scaffold at this stage will easily be disintegrated in culture medium as no strong linking among waterborne polymer particles is established. Thus, the autohesion or inter-particle polymer chain diffusion is necessary to be developed in the final coalescence step.[24] As latex coalescence ensues, the strength of

the scaffold becomes correlated to the extent of coalescence, which is, in turn, largely controlled by the difference between the process temperature (T_p) and the glass transition temperature (T_g) of the polymer particles. If $T_p << T_g$, the polymer chain diffusion from one particle to another will be difficult to advance and mechanical prosperities of the scaffold can not be developed; at the other extreme $T_p >> T_g$, the healing of particle boundary is fast and a coherent and continuous solid will readily form. Thus, to obtain desirable mechanical properties in colloidal gel based techniques, T_p should be comparable to or higher than the T_g of the latex polymer particles in the colloidal gel.

Due to the sensitivity of the protein-based growth factors or other bioactive molecules, the process temperature cannot exceed 37 ^{o}C either in the short or long term. For many biodegradable polymers with a low T_g, such as poly(ε-caprolactone) (PCL, T_g = –66˚C), polyhydroxyalkanoate (PHA, T_g = 4˚C**),** polypropylene Fumarate (PPF, T_g = –10˚C), the corresponding colloidal particles can be used directly in this process. According to PLA, PGA, and their copolymer PLGA, whose T_g range from 35 ^{o}C to 65 ^{o}C,[127] adjustment of their T_g by adding plasticizers or copolymerizing with low T_g polymers may be used. For example, the T_g of the PLGA (85:15) colloidal particles decreases sharply from 48 ^{o}C to 27 ^{o}C by adding 10 % PEG 1500.[128] Consequently, the formulated PLGA colloidal gels can then be processed into scaffold and aged to develop a high mechanical integrity.

The polymer binder is critical for the colloidal gel formation and, preferably, two mechanisms can be utilized to induce the colloid-gel transition in a colloidal suspension. One is to collapse the extended binder (i.e. stabilizer) layers adsorbed on particle surface to induce flocculation and the other is to form the inter-particle bridging by cross-linking adsorbed binder on particle surface. Thus the binder should have the ability to transform

conformation either under the change of environmental factors (solvent pH or temperature) or cross-link by themselves or with other substances. It should be cognizant that the crosslinking must be reversible so that the particle network in the colloidal gel can be broken under high shear and re-establish after removal of the shear. Therefore, crosslinking of the polymer binder should be formed through non-covalent bonding physical forces, such as ion bonding, van der waals forces, hydrophobic bonding, and so on. The examples of these gelling polymers include thermoresponsive polymers (agar, agarose, kappa carragreenan and pluronic), pH dependent polymers (polyacrylic acid), and ionic interaction pairs (alginate + calcium ion, alginate + chitosan, polyacrylic acid + Polyethyleneimine). Other important requirements for the polymer binder include that they should be biocompatible, non-toxic, and biodegradable in some circumstances.

3.4 Conclusions

The use of colloidal materials to print 3D scaffolds offers several new directions for tissue engineering. First, solid freeform fabrication of combined synthetic and natural polymers is achievable in the same scaffold due to the modular material design. Second, because of the aqueous and low temperature nature of the process, bioactive molecules may be readily incorporated into the material for subsequent drug release and biological signaling. Third, the scaffolds fabricated can be used directly without extensive and laborious purification post-printing steps. These features may make scaffolds derived from printing of colloidal gel materials attractive as tissue engineering scaffolds for a variety of applications where pore size control and drug delivery capabilities are desired. The

printing process also enables the possibility of functionally graded structures where drug concentrations may be heterogeneously distributed throughout the scaffold.

Chapter 4 Controlled Release System

4.1 Introduction

The tissue development and functions are vitally dependent on encouragement of the cells to proliferate, differentiate, migrate, and interact with each other. All these critical cell behaviors are largely regulated through the interplay of a variety of protein based message molecules, including large families of growth factors and cytokines.[1, 129, 130] To facilitate the therapeutic effectiveness of the regenerated tissues, there is an increasing awareness of the need to delivery these signaling factors that mimic their endogenous production profiles to the target cell population. However, once administered, the circulatory half-lives of these growth factors are short compared to the time required for cell response.[131, 132] Hence, incorporation of labile proteins in bioscaffolds and controlled delivery has been extensively adopted in tissue engineering.[133, 134] In addition to the demand for the temporal availability of the biological factors, the ability to create concentration gradients of growth factors in three dimensions is even more important to optimize and speed organogenesis. To date, current therapies to regenerate a variety of tissues are restricted to the bolus delivery of single growth factor in the entire tissue culture environment, which may not be the ideal approach to drive the growth of functionally heterogeneous cells toward highly spatially organized arrangement for tissues regeneration.

The applications of aqueous polymer latex dispersions in pharmaceutical controlled release formulations have rapidly increased during the past few years.[135, 136] The mechanism for the controlled release relies on the formation of diffusion retardant membrane or matrix from aqueous latex such that the drug will be released from a reservoir.

However, protein agents present a challenge for aqueous latex dispersion based controlled release system as proteins were considered too large to slowly release from the non-erodible hydrophobic polymers by Fickian diffusion mechanism.[81] On the other hand, protein controlled release technology based on hydrogels, three-dimensional hydrophilic polymeric networks capable of imbibing large quantities of water, has generated a lot of interest.[131] These systems offer a 'protein-friendly' environment for the delivery of biologically active molecules and the protein release rate can be controlled by of many mechanisms, such as dissolution for physically entangled hydrogel and hydrolysis or degradation for chemically crosslinked system.[137] Nevertheless, the hydrogels are normally weak in physical strength, which limited their application in tissue engineering.

As demonstrated in last chapter, we have developed a novel direct write technique to fabricate tissue engineering scaffolds based on polymer colloidal gels, which is a class of materials consisting of a percolating network of attractive latex particles.[138] We hypothesize that the distinctive structure of the colloidal gels will allow them to form protein release vehicles with both hydrogel-like protein friendly environment and suitable mechanical integrity of the latex systems. Beside, the unique viscoelastic behaviors of the colloidal gels will make them ideally suitable for assembling arbitrary three-dimensional (3D) components capable of spatially controlled growth factor delivery.[106, 109-112, 115-122] In this study, strategies were developed to incorporate the proteins in the scaffold to realize the localized and sustained delivery. First, we incorporated model protein, bovine serum albumin (BSA), into the acrylic based colloidal gels and fabricate them into porous scaffolds. To further extend the duration of protein release, we also created composite colloidal gels for scaffold fabrication by dispersing BSA encapsulated chitosan

nanoparticles in bare colloidal gels. Platelet-derived growth factor (PDGF) was selected as a model growth factor and its bioactivity was assayed after release from the scaffolds to investigate the protein stability after incorporation. Based on this platform, we also explored the possibility to create a functional equivalent of lymphoid tissue by generating a heterogeneous scaffold capable of incorporating multiple chemo-attractant (or cytokines) and subsequently release to localize lymphocytes and dendritic cells within the artificial tissue and finally elicit a desirable immune response.

4.2 Materials, Methods and Modeling

4.2.1 Material System

Bovine serum albumin (BSA) and tripolyphosphate (TPP) were purchased form Sigma-Aldrich and used as received. Chitosans (Sigma-Aldrich) of medium viscosity (200-800 cP) were purified by filtration its solution on glass fiber to remove the insoluble substance and de-polymerized to fragments with various molecular weight through sodium nitrite degradation.[139] Lyophilized rat recombinant PDGF-BB (R&D system, Minneapolis, MN, USA) was reconstituted in HCl solution (0.5 mM, pH = 4.3) with 0.1 *wt*% BSA to a concentration of 0.2 mg/ml.

4.2.2 Protein Incorporation

The strategy here to make protein incorporated colloidal gel is to first formulate the bare colloidal gel as the base material and then disperse the proteins through mixing, either in their original forms or nanoparticle embedded forms. To prepare protein incorporated colloidal gels, the calculated amount of model proteins or protein encapsulated

nanoparticles were added to bare colloidal gels (prepared according to the protocol described in Chapter 3) and mixed for 10 min at room temperature using a home-built syringe mixer.[140] In all the cases, the protein loadings are kept with 0.5 *wt*%.

BSA encapsulated chitosan nanoparticles were prepared according to the protocol reported before.[104, 141] Briefly, chitosan of various molecular weights along with BSA were dissolved in 1 *wt*% acetic aqueous solution at concentration of 1 mg/ml and 0.5 mg/ml, respectively. Then 2 ml of 1.0 mg/ml TPP solution was added to 5 ml of the chitosan-BSA solution. Nanoparticles were formed spontaneously under magnetic stirring at room temperature due to ionotropic gelation between chitosan and TPP. The suspension was kept magnetic stirring for 30 min and the nanoparticles were collected by ultracentrifugation at 20000×g.

4.2.3 Scaffold Fabrication

The scaffolds were robotically assembled by extruding the protein loaded colloidal gels as described in Chapter 3. All scaffolds were fabricated in cuboid shape with a measuring of 2 mm× 1.2 mm ×0.9 mm. 150 μm nozzles and a deposition speed of 5 mm/s are used in the assembly of these structures. In all the cases, the rod spacing in each layer was fixed at 300 μm and the layer spacing was kept with $\Delta z = 0.95D$.

Immediately after deposition, the scaffolds derived from colloidal gels were dried and hardened in a dry incubator at a constant temperature of 37 ^{o}C for at least 1 hour. The scaffold drying kinetics was obtained by weighing the scaffold at various time points. To arrest the further particle deformation and coalescence, the processed scaffolds were stored in a –30 ^{o}C freezer. Stiffened scaffolds were freeze fractured in liquid nitrogen and

observed under the scanning electron microscope (SEM) to assess the internal structure and the gross morphology.

To investigate the protein distribution after incorporation, Texas Red fluorescent dye conjugated BSA was mixed with colloidal gels (1 *wt*%) and fabricated into scaffolds. The samples were first frozen in a - 30 ^{o}C freezer overnight. Then the scaffolds were embedded in a tissue-tek compound (OCT 4583, Sakura, Torrance, CA, USA) and spray frozen with coolant (Frostbite, SurgiPath Medical Industry, Richmond, IL, USA). To reveal the radial distribution of BSA, 10 μm thick cryostats were cut parallel to layer stacking direction in serial sections by a Cryo-Microtome (Jung FrigoCut 2000N, Leica Microsystems, Bannockburn, IL) and transferred to microscope slides. The slides were air-dried and then examined by an optical microscopy in fluorescence mode.

4.2.4 in vitro Protein Release

To characterize the release of a model protein, BSA loaded colloidal gel and colloidal gel-nanoparticles scaffolds were incubated in 5 ml 1× PBS solution at 37 ^{o}C and kept shaking at 100 rpm. The supernatants were fully recovered and same amount of fresh medium was added at each predetermined time intervals up to 7 days. The resulting samples were then analyzed for total protein content by a MicroBCA protein assay kit (Pierce, Rockford, IL, USA) and the amount of BSA released per scaffold was calculated using a standard curve.

To validate the bioactivity of released model growth factor, PDGF-BB incorporated scaffolds were fabricated with the identical protocol as for model proteins, except the PDGF-BB loading was controlled at about 200 μg per scaffold. To quantify actual growth

factor release, PDGF-BB scaffolds were precisely weighed and incubated in 1 ml Dulbecco's modified eagle's medium (DMEM) at 37 ^{o}C. The supernatants were fully recovered and same amount of fresh medium was added at each time point up to 14 days. Enzyme-linked immunosorbent assay (ELISA) to detect PDGF-BB release was performed using a standard rat PDGF-BB kit (R&D system, Minneapolis, MN, USA) and the amount of PDGF-BB released per scaffold was calculated using a standard curve.

4.2.5 Bioactivity Evaluation

PDGF-BB has been demonstrated as a chemoattractant on fibroblasts[142-144] and this chemotactic effect was used to evaluate the bioactivity for released samples from scaffolds. The cell migration assay for quantitation of the bioactivities of released growth factors was performed in ChemoTX plates (Neuro Probe, Gaithersburg, MD, USA) as described previously.[145] In brief, Swiss mouse embryo fibroblasts (NIH 3T3, ATCC) cells were labeled with fluorescence markers by rinsing twice with hanks balanced salt solution and then incubating in tissue culture flaks for 20 min with carboxy-fluoroscein succinimidyl ester (CFSE,10 μM).[146] This medium was then discarded and cells were washed once with DMEM with 10% fetal calf serum (FCS), once with DMEM alone and finally incubated overnight in DMEM alone. The following day, the serum-starved cells were trypsinized and re-suspended in serum-free medium (DMEM medium containing 5 *wt*% BSA) at a concentration of 1×10^{6} cells/ml. The ChemoTX plate with pore size of 5 μm was chosen and the experiment was conducted according to manufacturer's instructions. The medium containing released PDGF-BB was carefully transferred in the microplate wells. The fresh prepared PDGF-BB solution as positive controls and medium with blank scaffold soaked as

negative control were also added. Equal amounts of cell suspension (30μl) were loaded onto the filters at each site and the migration plate was incubated at 37 ^{o}C in a humidified atmosphere containing 5% CO_2 for 4 h. Migration of cells through the insert membrane was assessed by measurement of cellular CFSE fluorescence using a fluorescence plate reader with excitation and emission wavelength of 485 and 530nm, respectively.

4.2.6 Theoretical Modeling

First we assume that the contact points between layers can be omitted, so the scaffold can be regarded as a long folded rod (rod length >> rod diameter) and further approximated as an infinite cylinder. Thus the release from scaffold can then be considered as one-dimensional radial diffusion case in macroscopic scale, as illustrated in Figure 4.1. As the latex particles comprising the matrix of the polymer rod are impermeable to the protein, the protein transport occurs exclusively within aqueous Pluronic hydrogel filled pores. Also we assumed that the porosity kept unchanged during the whole delivery course.

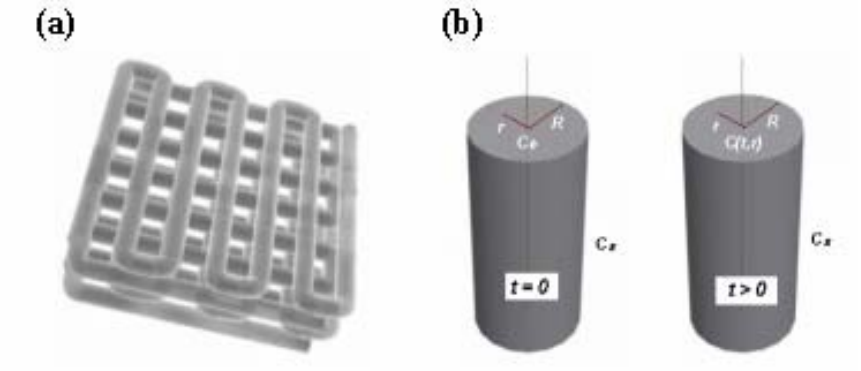

Figure 4.1. The drug release from scaffold can be considered as release from infinite cylinder. (a) 3D drawing of the scaffold; and (b) schematic of diffusion from infinite cylinder.

For the infinite cylinder subjected to a sink condition at $r = 0$, R, the mathematical formulation may be written as:

$$\frac{\partial C_p(t,r)}{\partial t} = D_e \frac{1}{r}\frac{\partial}{\partial r}(r\frac{\partial C_p(t,r)}{\partial r}) \tag{4.1}$$

with the initial conditions

$$C_{p,0} = C_p(t=0,r) = \frac{M}{\varepsilon\pi R^2 l} \tag{4.2}$$

and boundary conditions

$$C_p(t,r=-R) = C_p(t,r=R) = 0 \tag{4.3}$$

where $C_p(t,r)$ is the concentration of protein within Pluronic hydrogel filled pores at r and time t, D_e effective diffusion coefficient, r the radius of the cylinder, R the radius of scaffold rod, ε the porosity in the rod, and M the mass of protein originally incorporated into the inner rod pores and. The equation was solved in Maple and the solution is:

$$C_{hg}(t,r) = \frac{M^*}{\varepsilon\pi R^2 l}\sum_{n=0}^{\infty}\frac{4(-1)^n \exp\left(\frac{-\frac{1}{4}(2n+1)^2\pi^2 D_e t}{R^2}\right)\cos\left(\frac{\left(n+\frac{1}{2}\right)\pi}{R}\right)}{(2n+1)\pi} \tag{4.4}$$

The cumulative drug release at time t may be computed by

$$M_t = \int_0^t -2\pi R l \varepsilon \frac{\partial C_{hg}}{\partial r}\Big|_{r=R} dt \tag{4.5}$$

Combine Equation 3.4 and 3.5 obtain

$$\frac{M_t}{M_\infty} = 1 - \frac{16}{\pi^2}\sum_{n=0}^{\infty}\frac{1}{(2n+1)^2}\exp\left(-\frac{D_e(2n+1)^2\pi^2 t}{4R^2}\right) \tag{4.6}$$

In addition, we should assume homogeneity of the inner pore distributed in the rod, thus constant ε. So the term D_e may be expressed by

$$D_e = K_r F D_p \tag{4.7}$$

where D_p is the diffusion coefficient of the protein in Pluronic hydrogel, F is the formation factor, which summarize the effect of pore geometry and topology on diffusion, and K_r is

the restriction factor, which accounts for the drug/wall interactions induced by hydrodynamic and/or electrostatic effects. In some cases, we can define F as

$$F = \frac{1}{\tau^2} \tag{4.8}$$

where τ is the tortuosity of the rod pore network, normally ranging 1.5~1.7 in aggregated colloidal particles.

To extend the duration of protein release, proteins were encapsulated in chitosan nanoparticles. The protein release from the chitosan particle carrier is mainly due to the disassociation of the crosslinked chitosan molecules and de-adsorption of proteins.[147, 148] Thus, by addition of a dissolution term, Equation 3.1 becomes:

$$\frac{\partial C_p(t,r)}{\partial t} = D_e \frac{1}{r}\frac{\partial}{\partial r}(r\frac{\partial C_p(t,r)}{\partial r}) + \frac{dC_p}{dt} \tag{4.9}$$

with the initial conditions

$$C_{p,0} = C_p(t=0,r) = 0 \tag{4.10}$$

and the dissolution term can be expressed as

$$\frac{dC_p}{dt} = k\phi_{cs}C_s \tag{4.11}$$

where k is the chitosan disassociation rate constant, C_s is the protein solubility in chitosan nanoparticles, and ϕ_{cs} is the weight percentage of the chitosan particle in colloidal gels. As the diffusion in hydrogel is far more rapid than the dissolution process of the chitosan particles, so we can neglect the diffusion term and regard system as the sole dissolution controlled process. Thus the percentage of the protein release with respect of time can be expressed as:

$$\frac{M_t}{M_\infty} = Kt \tag{4.12}$$

where K is the combined constant derived from k, C_s, and ϕ_{cs}. The results indicate that, theoretically, the colloidal gel-chitosan nanoparticles composite system has a zero order release behavior.

4.3 Results and Discussion

4.3.1 Protein Incorporation

Since the rod of the scaffold was assembled from latex particles and particle coalescence toward a continuous solid was arrested after drying, we presume that the porosity within the rods still exists. This speculation is partially confirmed by the morphological observation of the scaffold samples with extended stiffening treatment procedure (dried at 37 ^{o}C after 6 hours), as shown in Figure 4.2(a). The rod surface was found of granular look at high magnificence, suggesting that the polymer particles in the rod were still not fully deformed and interpenetrated with each other. As illustrated in Figure 4.2(b), this unique structure can be regard as a sintered particle network with Pluronic and protein distributed in the interstitial spaces. Thus, we conclude that the scaffold derived from colloidal gels has two levels of pore structure. The primary structure is the macroporosity encompassed by the lattice rod arrays while secondary structure refers to the microporosity in the scaffold rod, which is formed by the interstices of aggregated or sintered colloidal particle networks. The unique secondary structure presents us an interesting potential for the incorporation of proteins in scaffold where protein can be loaded by dispersing in the interstitial space of the latex particle network. Upon contact

with release medium, the water or medium will quickly fill the cavities inside the scaffold rod and swell the Pluronic polymers absorbed on the particles to form hydrogels. The interstices in the polymer rod matrix become filled with aqueous Pluronic hydrogel, which is both the carrier and transport medium for the proteins to get out of the scaffold via diffusion. Thus the scaffolds can be utilized as controlled delivery vehicles for proteins, as illustrated in Figure 4.2(c).

To reveal the protein distribution within the scaffold, Texas red labeled BSA was incorporated in a scaffold and a 5 micron thin section of scaffold was cut in the radial direction of the scaffold rod. Figure 4.3 shows the images of thin section of polymer scaffold rods by using light microscopy in bright field and fluorescence mode, and confocal microscopy. As opposed to non-uniform surface to the substrate distribution of additive in sintered polymeric colloidal films,[149] the BSA is, in general, uniformly distributed throughout the diameter in scaffold rod except few air bubbles entrapped inside. The BSA locally aggregation and radius compositional difference was not observed even underwent with drying and stiffen procures. This phenomenon can be attributed to the trivial mobility resulted from large molecular weight of the protein.

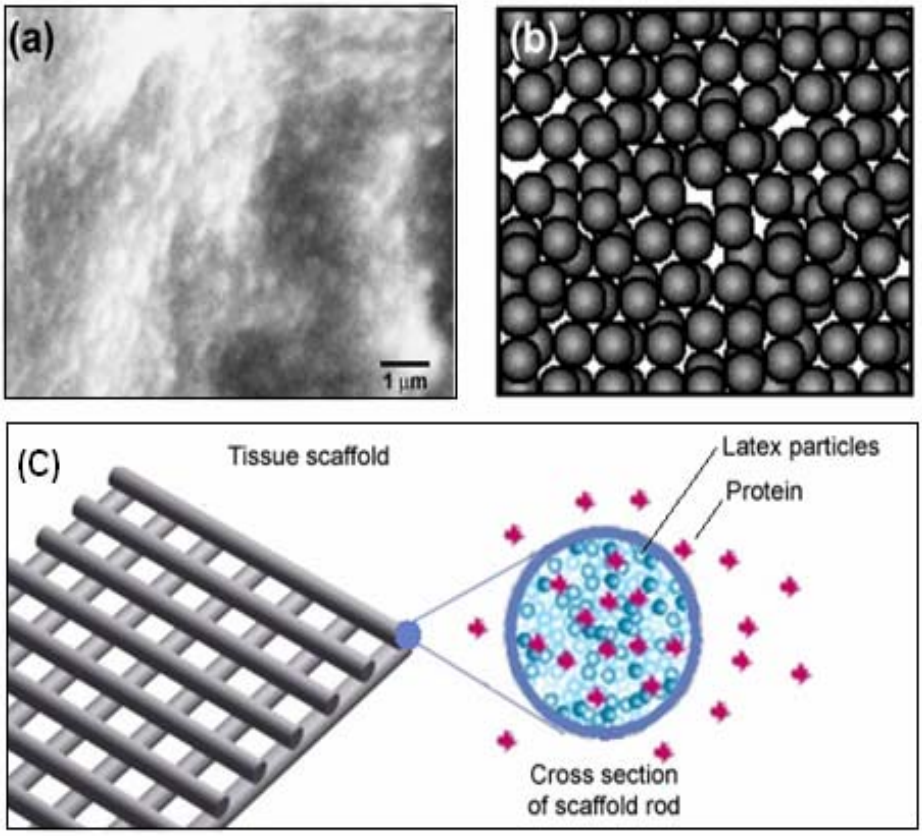

Figure 4.2. The colloidal gel based scaffold can be viewed as packed colloidal particles with particle sintering. (a) SEM photos of the surface morphology of the scaffold dried at 37oC after 6 hours; (b) schematic of packed colloidal particles; (c) schematic of two levels of scaffold structure and rationale of protein release from scaffold rod.

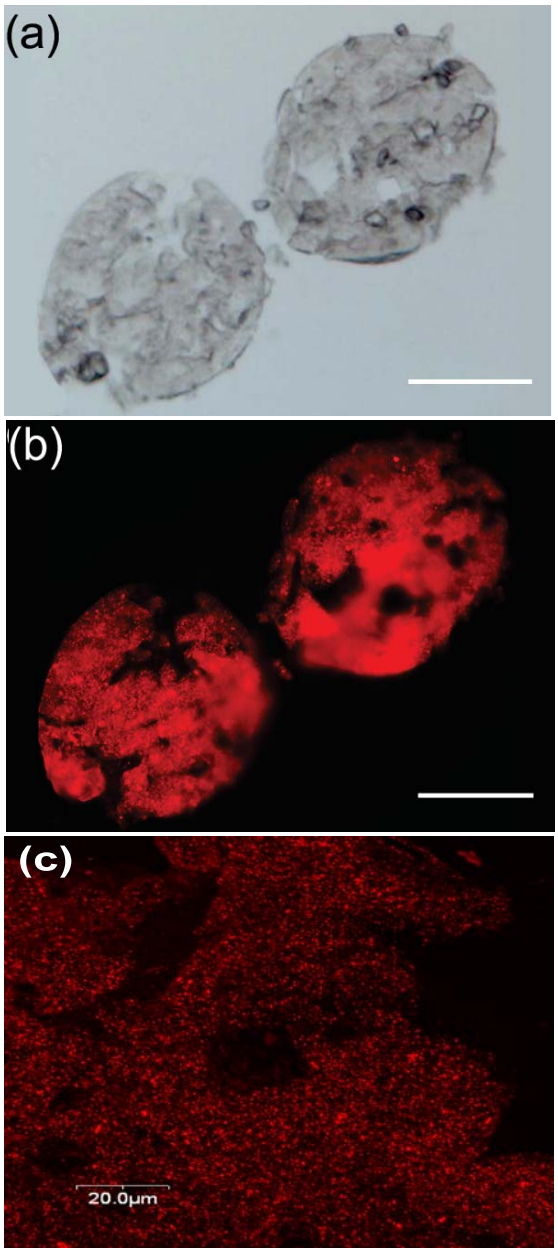

Figure 4.3. 5 micron thin section of the scaffold rod incorporated with Texas red tagged BSA protein imaged by light microscopy in (a) bright field mode and (b) fluorescence mode, showing the protein dispersed within the microporous structure of the scaffold rod. (c) Confocal microscopic image of scaffold rod cross section at a high magnification. The scale bars are 100 μm for (a, b).

4.3.2 Protein Release

BSA release behavior from colloidal gel derived scaffolds exhibited a strong dependence on post processing conditions. The effect of drying time on protein release was shown in Figure 4.4(a). The scaffold dried with 1 to 3 hours release nearly 60% of the total protein in 2 hours. After drying more than 3 hours, the protein release rate decreased notably and the scaffold dried with 6 hours released 60% of protein in 6 hours. The scaffold dried with 20 hours has the similar BSA release profile with scaffold dried with 6 hours, indicating that the further increase of drying time has no significant additional retardation effect on protein release. As evaporation of water from freshly deposited scaffold proceeds, the particles come closer together and a complex sequence of particle consolidation occurred due to latex deformation and particle inter-penetration.[22, 150, 151] The particle packing and scaffold densification cause not only the decreasing porosity but also the increasing tortuosity of the inner pore structure in the rod. The effect of varying tortuosity on release profile of the protein from scaffold was derived from Equation 4.6 and plotted in Figure 4.4(b). The trend of slower release with the increasing drying time is in accordance the simulated release profile, where the protein release rate was decreased with increasing of tortuosity. The BSA distributed in the interstitial pace of particle network has to take longer path in order to diffuse into the surrounding medium.

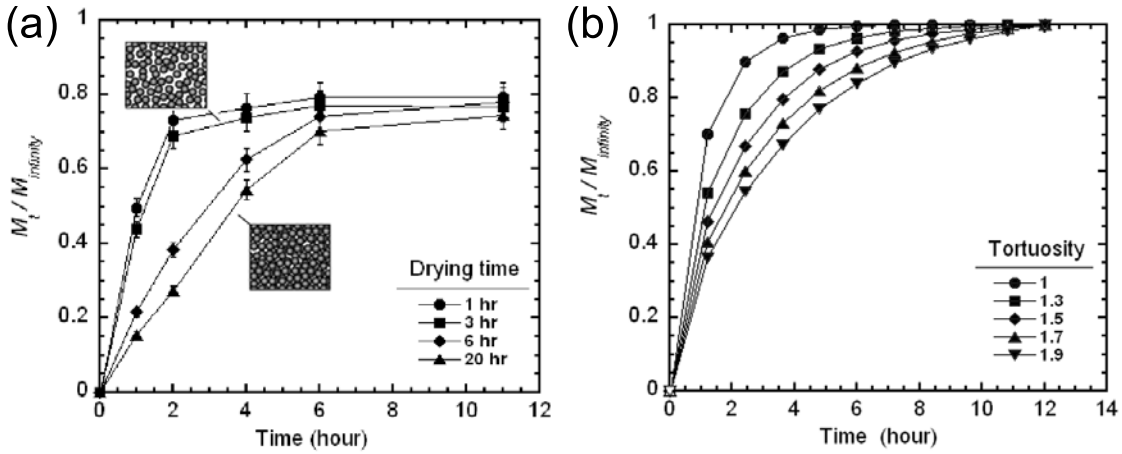

Figure 4.4. (a) The effect of drying time on BSA release profile; (b) simulated protein release profile from scaffold at various tortuosity, where D_p (about $3.40\times10^{-}8$ cm/s) was obtained from fitting of experimental data.

As the latex particles comprising the matrix of the polymer rod are impermeable to the proteins, the protein transport occurs exclusively within aqueous Pluronic hydrogel filled pores. Thus the protein diffusion behaviors in colloidal gel are mainly determined by protein diffusion coefficient in the Pluronic hydrogels. As shown in Figure 4.4(a), we observed that the release of BSA from colloidal gels is rapid and hydrogel in the scaffold rod has modest retardation effect on the protein diffusion: more than 60% released within 6 h in most cases. This result can be contributed to the larger mesh size of Pluronic hydrogel mesh size compare to the much smaller dimensions of protein molecules. Though the protein release behavior can be affected by the characteristics of the microporous structures, such as tortuosity and pore connectivity in the scaffold rod, these factors are difficult to control and may have adverse effect on scaffold structural and mechanical properties.

Recently, the controlled release of protein from hydrophilic nanoparticles, especially chitosan nanoparticles, has received much attention in therapeutic delivery field.[104, 147, 148] A major advantage of these nanoparticles is that they are synthesized under extremely mild

conditions and the protein bioactivity is usually maintained.[141] Besides, they provide a continuous release of protein for extended periods of time and the release profile can be readily modulated by molecular and formation parameters of particles. To extend the duration of protein release from the colloidal gel resulted scaffolds, protein was first encapsulated in chitosan nanoparticles and then admixed with colloidal gel to form a composite colloidal gel system for fabricating protein incorporated scaffolds. As the particle size of the synthesized chitosan nanoparticles is normally in the range of 50 to 300 nm, which are relatively smaller than the size of acrylic latex particles that formed the microporous structure of the scaffold rods, the addition of chitosan nanoparticles into the colloidal gels has no significant effects on the drying and stiffen behaviors of the derived scaffold, which has also been confirmed experimentally.

Figure 4.5 shows the BSA release profiles of the composite colloidal gel scaffolds with encapsulating chitosan of various MW. All the scaffolds exhibit two release phases, a rapid release over the first 5 hours followed by a slow release for up to 7 days. The first release phase could be contributed to the release of BSA that were lightly associated with chitosan molecules and located near the surface of the particles while the second phase might correspond to those BSA more efficiently entrapped and tightly bound to the chitosan particles. The BSA proteins release from composite scaffolds at a constant but different rate by varying chitosan MW. The higher the MW of the chitosan that made the nanoparticles, the faster the BSA release from the composite scaffold. Theses results indicate that it's possible to modulate the release rate of composite scaffold by simply adjusting the chitosan MW.

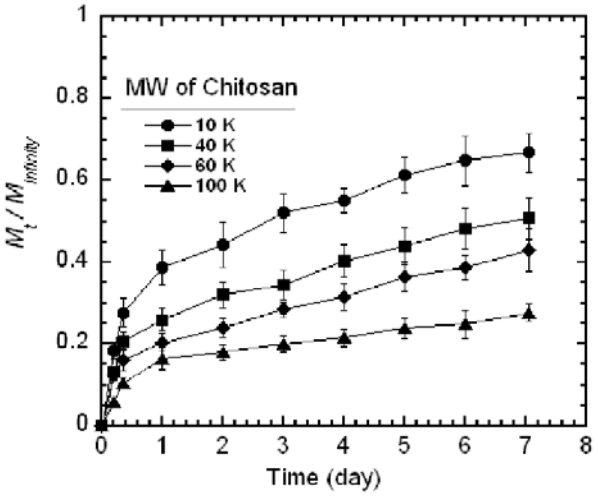

Figure 4.5. The BSA release profile of scaffold fabricated with colloidal gel-chitosan nanoparticles composite scaffolds with varying molecular weights of chitosan.

4.3.3 Stability Testing

The protein property is another important factor affects protein release behavior from the colloidal gel scaffold. Figure 4.6 shows the release profiles of PDGF-BB from both colloidal gel scaffolds and composite colloidal gel scaffolds. The result revealed that PDGF-BB could be persistently released for optimal therapeutic efficacy in tissue engineering applications. Compared to BSA, PDGF-BB exhibits a much slower and sustained profile when they directly incorporated in colloidal gels. PDGF-BB and BSA have a distinctive isoelectrical point (IEP): the IEP of BSA is about 4.9 while PDGF-BB has an IEP of 11.0, suggesting that electrostatic forces may play a role in the difference of their release behaviors. In neutral pH medium, the PDGF-BB become highly positively charged after hydration and has higher affinity to the Pluronic molecules. To diffuse out to the release medium, PDGF-BB must overcome more hindrance than BSA, which may account for the slower release.

The bioactivity of the released proteins from scaffold was assessed by assaying the chemotactic effectiveness of the released PDGF-BB growth factors, which is the indicator for the level of their bioactivity. The PDGF-BB incorporated scaffold was soaked in the medium. Samples were collected during the release period of day 2 to day 4 and then diluted to 10 ng/ml and 2ng/ml. The media soaked with bare scaffold alone were selected as the negative control. Standard PDGF-BB solutions of same concentration as samples were prepared as positive control. As shown in Figure 4.6, the number of migrated cells was charted at varying concentration of released PDGF-BB and standard solution. Higher degree of cell migration was observed from PDGF-BB solution in contrast to that from the negative control media. PDGF-BB release from colloidal gel and colloidal gel-chitosan nanoparticles composite exhibited almost the equivalent cell chemotaxis activity as compared to standard PDGF-BB at both the level of 2 ng/ml and 10 ng/ml. In addition, the result showed an increasing responsiveness of fibroblast cell to both released and standard PDGF at increasing concentration from 2 to 10 ng/ml. This found concentration dependent chemotaxis behavior is consistent to the previously finding.[145, 152] The result revealed that the released PDGF retains its original biological activity and the mild biocasting procedures exert trivial effect on PDGF stability.

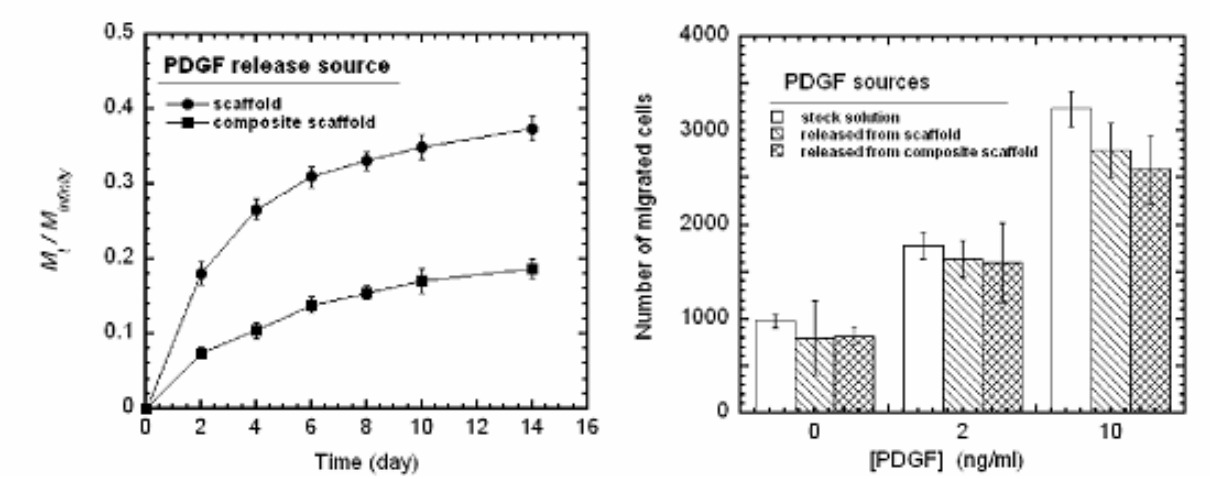

Figure 4.6. (a) Release profile of PDGF-BB loaded in colloidal gel scaffold and colloidal gel-nanoparticles composite scaffold. (b) Chemotactic activity of PDGF released from colloidal gel based scaffold. Chemotactic activity was determined as the amount of migrated cells.

As the scaffold fabrication process described in this work simply rely on the rheological properties of the colloidal material and the ability of the latex particles to coalescence upon drying with the application of minimal heat (typ. < 37 ^{o}C), thus the encapsulated protein will have little chance to get denatured. Furthermore, the constitute of the colloidal gel, Pluronic F127, has a unique stabilization effect to protein structure, makes it capable of preserving polypeptide bioactivities *in vitro* and *in vivo*.[153] This factors may all contribute to the great biological benign properties of the process

4.3.4 Spatial Control of Protein Release

The additive nature of the process and unique self-supporting feature of the colloidal gel offers great promise for producing objects made of multiple materials or functionally graded materials with complex internal void.[154] It provides a superb platform to fabricate heterogeneous scaffolds for complex artificial tissues, which require the spatial and temporal delivery of the biochemical signals to guild tissue growth and maintain cell

organization. In a typical process as illustrated in Figure 4.7, the multi-material deposition system fitted on the consists multiple material reservoirs (Figure 4.7 (a)) which house colloidal gel material loaded with different growth factors and feed to a common orifice or individual orifices. First, the designed 3D model is converted to a series of slices and then the outline of each slice is filled with some combination of contouring and rastering to produce a written path, which is also assigned a material property derived value. The position and material information is written into an interchangeable XML file and output via a machine specific script files, telling the writing machine to set syringe moving speed, deposition rate, dispensing on-off and so on. By controlling the relative flow rates of the multiple material feeds, the composition of the extrudate can be easily varied. Using this approach, an arbitrary-shaped 3D tissue construct with linear or non-linear composition gradients can be fabricated.

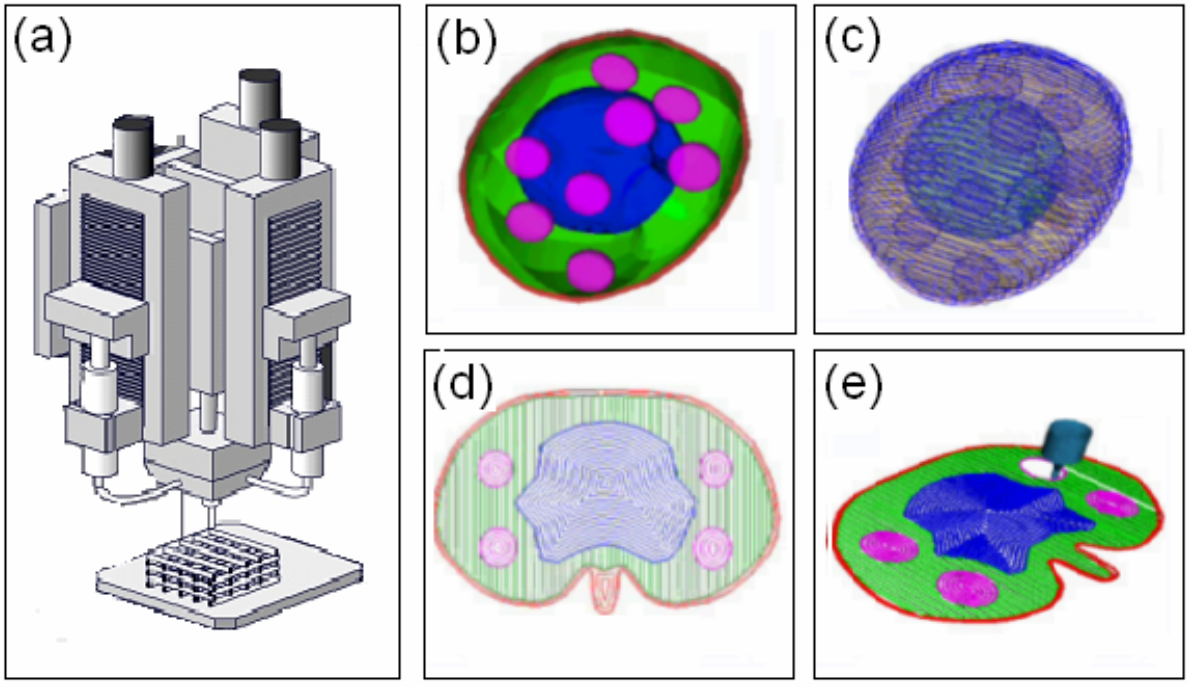

Figure 4.7. (a) A multi-material deposition system fitted on the consists multiple material reservoirs. The heterogeneous scaffold can be fabricated with a typical information

system process: (b) establish a 3D model; (c) model slicing into multiple layers; (d) generate filling toolpaths; (e) simulated deposition with multiple materials.

4.3.5 Artificial Lymph Node

In this work, our endeavors have been focus on developing a tissue equivalent of lymph node (artificial lymph node) for drug and vaccine testing. As it is a gigantic challenge to fabricate tissue constructs that faithfully replicate the natural lymph node morphologically and capable of regulating the cellular behavior in the exact tissue hierarchy, we hypothesize that, by coaxing the lymphocytes to form the essential organization as in the living tissue, a functional equivalent of a lymph node could be accomplished that possess the equal tissue functions as the real lymph node. As exhibited in Figure 4.8, lymphoid tissues exhibit a unique histological structure or 3D architecture comprising of an assortment of functionally distinct zones.[155] Notably in the lymph node, the physical segregation of T and B lymphocytes zones is believed to facilitate the T-B cell migration and interaction, implying its significance in the mediation of the of lymphocytes interactions, maturation and migration, and finally a efficient immune reactivity.[156, 157]

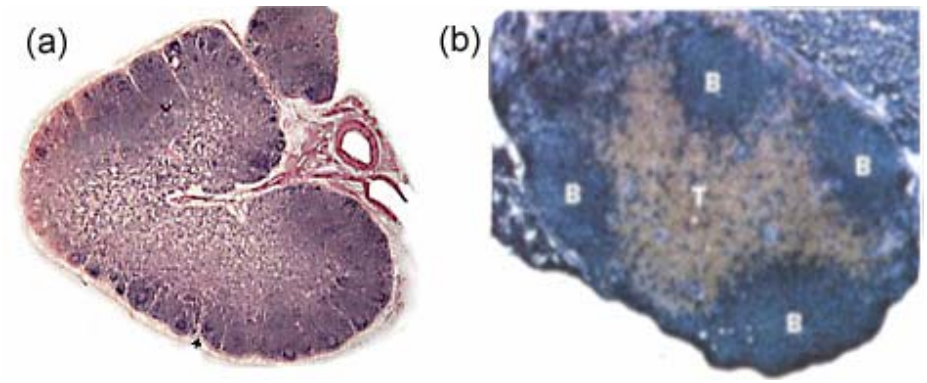

Figure 4.8. (a) Histological section of the lymph node and (b) example histology of lymph node where B cells are stained blue and T cells brown.

Base on this assumption, the potential application of fabricated scaffolds for lymphoid tissue equivalent was investigated. As the cell signal communicating proteins can be readily integrated to colloidal gel material and controlled release without loss of bioactivity, it become viable to incorporate appropriate cytokines in the scaffold and strategically controlled release in geospatial variation mode to stimulate T and B cells form the T and B cell zone organization. Among large families of chemokines and chemotactic agents that regulate the migratory pathways of immune cells, CXCL13 for localizing B cells and CCL19 and CCL21 for attracting T and dendritic cells, are believed be a key to maintain the highly motile T and B lymphocytes within the distinctive zones. For the proof of concept demonstration (Figure 4.9), a heterogeneous scaffold was assembled with one material incorporated with CXCL13 for localizing B cells and the other one integrated with CCL19 and CCL21 for attracting T and dendritic cells. The prototyped scaffold has a unique checkerboard pattern to mimic the tissue architecture and extracellular signaling environment seen by lymphocytes. In the design, every unit includes eight interconnected pores in the dimension of about *150* μm and is surrounded with straight channels, which may help facilitate the nutrient transportation and cell migration, ultimately simulating T and B cell organization sufficiently to achieve appropriate tissue functions.

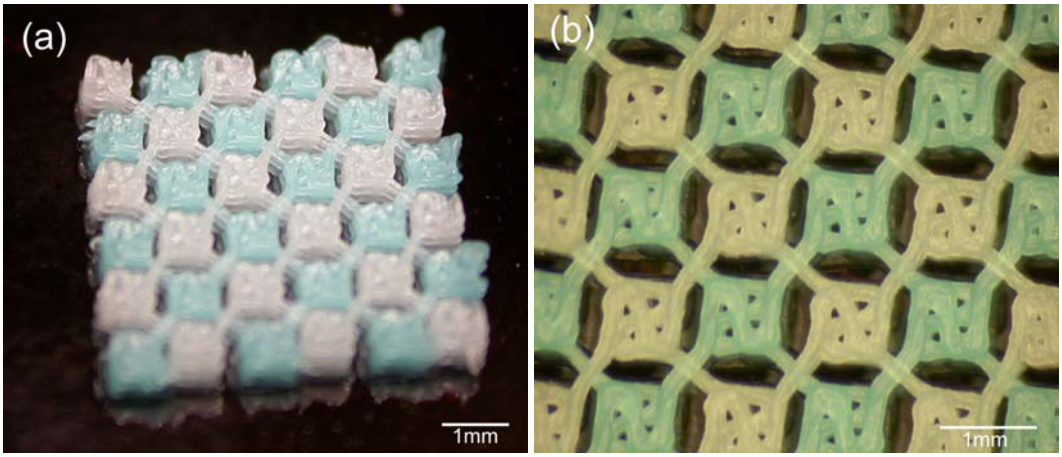

Figure 4.9. Heterogeneous scaffold deposited with perpendicular serpentine pattern for artificial lymph node. (a) Photo of freshly deposited scaffold and (b) microscopic picture showing segregated zones with distinctive colors.

Based on this multiple cytokine release scaffold that mimic the local environment of the lymph node, the formation of artificial lymph node will finally promising. Nevertheless, the more experiments (i.e. investigation of appropriate cytokine loading effect on cell localization) need to be done to further prove the viability of this scheme.

4.4 Conclusions

In this work, strategies for incorporation of proteins into colloidal gel based scaffold and subsequently releasing in a temporally and spatially controlled fashion have been developed. In the first method, the model protein BSA was admixed directly with colloidal gels such that they can be dispersed in the interstices of colloidal particle networks. However the protein release from resulting scaffold was rapid and difficult to control. To achieve a sustained release system, the protein was encapsulated in chitosan nanoparticles first and then dispersed in colloidal gels. The resulting composite colloidal gel scaffold was shown extended the duration of protein release to more than one week and the release rate

can be controlled by adjusting molecular weight of chitosan molecules. Additionally, the protein retains its bioactivity after release, which is confirmed by cell chemotaxis assay. In this work, the approach for spatial control of protein release was also demonstrated. Based on this platform, a checkerboard patterned heterogeneous scaffold was designed and fabricated to demonstrate the possibility for forming an artificial lymph node.

Chapter 5 Conclusion and Recommendations

5.1 Conclusions

The following is a summary of the tasks that were performed and the conclusion of the studies conducted.

1. The colloidal gels were formulated by combining polyacrylate latex particles with Pluronic F127 copolymers as binder, which are conjectured to adsorb such that the hydrophobic PPO section in the middle anchors on the particle surface whereas the solvated PEO blocks extend out into the solution. With appropriate formulation parameters, the extending PEO strands from neighboring particles become crosslinked through hydrogen bonding and finally lead to colloidal gels.

2. The viscosity and elastic modulus of colloidal gel are a function of Pluronic volume fraction. At $\phi_{Pluronic} < 0.05$, the colloidal gels displayed only weak shear thinning and a negligible yield stress while, at $\phi_{Pluronic} > 0.06$, the colloidal gels strengthened and exhibited a significant pseudoplastic and thioxtropic behavior, which can be described by the Hershel-Bulkley model.

3. The viscoelastic and rheological properties of colloidal gel are also dependent on solid loading. η_{app} and G' increase with increasing of $\phi_{particle}$ for the colloidal gels, especially the yield stress increases more than 10 fold with $\phi_{particle}$ from 0.50 to 0.55. With $\phi_{particle} = 0.62$, the system approaches the maximum solids loading and processing become extremely difficult.

4. The colloidal gels initiated by physical association become temporarily disrupted when subject to high shear conditions such as deposition and so as to exhibit a shear thinning rheology. Upon returning to a quiescent state, the colloidal network is re-established rapidly and the material returns to the gel state. This unique feature of colloidal gels is well suited to fulfill the requirements of flow through a deposition nozzle and rapidly "set" to maintain the shape of the deposited structure.

5. Scaffolds with periodic lattice structure of tetragonal and cylindrical symmetry were assembled from colloidal gel based materials. The scaffold rods maintained a circular cross section and spanned the gaps with minimal deflection after deposition. The feature size of the process is mainly dependent on material properties and nozzle size, normally in the range of 100~200 μm. The porous structure of scaffolds can be controlled by varying deposition parameters. Scaffolds with a porosity from 0.23 to 0.86 have been successfully fabricated.

6. GFP transfected quail mesodermal stem cell (QCE6) was seeded into the tissue scaffolds. During the culture, cells were seen to attach onto the scaffold surface, actively grow in the pore structure, and finally occupy the entire scaffold in three dimensions. The cytotoxicity of the scaffold materials was assessed by GFP expression of the QCE6 cell in scaffold. The result demonstrates the ability to culture cells on the scaffold while maintaining viability of the cells over the 14-day period, suggesting minimal cytotoxicity of the scaffold material to quail stem cell line.

7. The solidification of colloidal gel based scaffolds is governed by the glass transition temperature (T_g) of the polymer particles in the contact zone. If process temperature (T_p) >> T_g , the colloidal gels will readily to sinter and form a coherent and continuous solid.

8. As the particle coalescence toward a continuous solid was arrested after drying, the derived scaffolds have a secondary structure formed by the interstices of aggregated or sintered colloidal particle networks. This presents us an interesting potential for the incorporation of proteins in scaffold where protein can loaded by dispersing in the interstitial space of the latex particle network.

9. The cross sections of the polymer scaffold incorporated with Texas red labeled BSA were examined by light and confocal microscopy and shown the BSA is uniformly distributed throughout the diameter in scaffold rod with no locally aggregation and radius compositional difference. This phenomenon was attributed to the trivial mobility resulting from large molecular weight of the protein.

10. BSA release behavior from colloidal gel derived scaffolds exhibited a strong dependence on post processing conditions, such as drying time. The protein release rate of scaffold decreased notably with longer drying. This phenomenon was attributed to particle packing and scaffold densification and the resulting extra tortuosity of the inner pore structure in the rod.

11. In the cases that BSA is incorporated into scaffolds with original form, the rapid protein release was observed, suggesting that Pluronic F217 hydrogel in the scaffold rod has minor retardation effect on the protein diffusion. This result can be contributed to the larger mesh size of hydrogel mesh size compare to the much smaller dimensions of protein molecules.

12. To extend the duration of protein release from the colloidal gel resulted scaffolds, a colloidal gel-nanoparticle composite system was implemented by encapsulating protein in chitosan nanoparticles and then admixing nanoparticles with colloidal gels. The BSA

proteins release from composite scaffolds at a sustained profile and constant rate. Also the protein rate is dependent on chitosan MW. The higher the MW of the chitosan that made the nanoparticles, the faster was the BSA release from the composite scaffold.

13. To investigate the stability of the incorporated proteins, the chemotaxis behavior of growth factors was chosen as the indicator for the level of their bioactivity. PDGF-BB release from colloidal gel and colloidal gel-chitosan nanoparticles composite exhibited almost the equivalent cell chemotaxis activity as compared to standard PDGF-BB at both the level of 2ng/ml and 10 ng/ml. The result revealed that the released PDGF retains its original biological activity and the mild biocasting procedures exert trivial effect on PDGF stability.

14. The additive nature of the process and unique self-supporting feature of the colloidal gel offers great promise for producing objects made of multiple materials or functionally graded materials with complex internal void. By controlling the relative flow rates of the multiple material feeds, the composition of the extrudate can be easily varied. Using this approach, an arbitrary-shaped 3D tissue construct with linear or non-linear composition gradients can be fabricated

15. The potential application of fabricated scaffolds for lymphoid tissue equivalent was investigated. As the physical segregation of T and B lymphocytes zones is believed to have its significance for the efficient immune reactivity, a heterogeneous scaffold was assembled with one material incorporated with CXCL13 for localizing B cells and the other one integrated with CCL19 and CCL21 for attracting T and dendritic cells.

5.2 Recommendations

It is strongly encouraged that continued investigation need to be done to further prove the viability of this scheme.

1. Formulation of colloidal gels for better mechanical and biological properties using different latex polymer and binders. Develop polymer nano/micro particle manufacturing techniques to fabricate various candidate latex polymers into particle with desirable size and size distributions. Evaluate various physical associative polymers as binder, such as collagen, chitosan and agar, and develop different gelling methods with respect to various binder properties.

2. Evaluate the interaction between colloidal gels and seeded cells. Screen materials by performing the lymphocyte culture in the scaffold for excellent biocompatibility and minimal immunogenicity.

3. Incorporate appropriate cytokines in the scaffolds and strategically controlled release in geospatial variation mode to stimulate T and B cells form the T/B cell zone organization. Investigate the appropriate cytokine loading effect on cell localization.

Reference

1. Bell, E., *Tissue engineering in perspective*, in *Principles of tissue engineering*, R.P. Lanza, R.S. Langer, and J.P. Vacanti, Editors. 2000, Academic Press: San Diego.
2. Vacanti, J.P. and R. Langer, *Tissue Engineering.* Science, 1993. **260**(5110): p. 920.
3. Mooney, D.J., et al., *Principles of tissue engineering and reconstruction using polymer-cell constructs.* Mater Res Soc Symp Proc, 1992. **252**: p. 345.
4. Hutmacher, D.W., *Scaffolds in tissue engineering bone and cartilage.* Biomaterials, 2000. **21**: p. 2529-43.
5. Freed, L.E., et al., *Biodegradable polymer scaffolds for tissue engineering.* Biotechnology, 1994. **12**: p. 689-693.
6. Whitaker, M.J., et al., *Growth factor release from tissue engineering scaffolds.* J. Pharm. Pharmacol., 2001. **53**(11): p. 1427.
7. N. Wang, J.P.B., D.E. Ingber, *Mechanotransduction across the cell surface and through the cytoskeleton.* Science, 1993. **260**(1): p. 124-7.
8. A.G. Mikos, G.S., S.M. Leite, J.P. Vacanti, R.S. Langer, *Laminated three-dimensional biodegradable foams for use tissue engineering.* Biomaterials, 1993. **14**(5): p. 323-30.
9. D.J. Mooney, L.G.C., R. Langer, L. Johnson,L.K. Hansen, D.E. Ingber, J.P. Vacanti, *Principles of tissue engineering and reconstruction using polymer-cell constructs.* Mater. Res. Soc. Symp. Proc., 1992. **252**(345).
10. D. W. Hutmacher, S.H.T., I. Zein, K. W. Ng, J. T. Schantz and J. C. Leahy, *Design and fabrication of a 3D scaffold for tissue engineering bone.*, in *Synthetic Bioabsorbable Polymers for Implants*, J.E.P.a.S.T.L. C. M. Agrawal, Editor. 2000, American Society for Testing and Materials: West Conshohocken. p. 152-167.
11. C. Steidle, D.K., R. Chartoff, G. Graves and N. Osborne. *Automated fabrication of custom bone implants using rapid prototyping.* [http://www.udri.udayton.edu/rpdl/papers.htm] 1999 [cited.
12. S.S. Kim, H.U., J.A. Koski, B.M. Wu, M.J. Cima, J. Sohn, K. Mukai, L.G. Griffith and J.P. Vacanti, *Survival and function of hepatocytes on a novel 3D synthetic biodegradable polymer scaffold with intrinsic network of channels.* Annual Surgery, 1998. **228**: p. 8-13.
13. K.K. Uwe, B.B., A. Carsten and J. Valk. *Creating of bio-compatible high stress resistant and resorbable implants using multiphase jet solidification technology*. in *Time-Compression Technologies '98 Conference*. 1998. Nottingham, UK: Rapid News Publ, London.
14. Shaw, D.J., *Introduction to Colloid and Surface Chemistry*. 4th. ed ed. 1992, Boston: Butterworth-Heinemann. 1-20.

15. Fitch., R.M., *Polymer Colloids: A Comprehensive Introduction*. 1997, San Diego, Calif.: Academic Press.

16. I. D. Morrison, S.R., *Colliodal dispersions, suspension, Emulsion, and foams*. 2002: John Wiley & Sons, Inc. 374.

17. Lewis, J.A., *Colloidal Processing of Ceramics.* J. Am. Ceram. Soc, 2000. **83**(10): p. 2341-59.

18. Derjaguin, B. and L. Landau, *Theory of the Stability of Strongly Charged Lyophobic Sols and of the Adhesion of Strongly Charged Particles in Solutions of Electrolytes.* Acta Physicochim. URSS, 1941. **14**: p. 633-52.

19. Derjaguin, B., Trans. Faraday Soc., 1940. **36**: p. 203.

20. Overbeek, E.J.W.V.a.J.T.G., *Theory of the Stability of Lyophobic Colloids*. 1948, Amsterdam: Elsevier.

21. P.J. Flory, a.W.R.K., *Statistical mechanics of dilute polymer solutions. II.* J. Chem. Phys., 1950. **18**: p. 1086-94.

22. J. W. Vanderboff, E.B.B., W. K. Carrington, *Transport of water through latex films.* J Polym. Sci., Polymer Symposia, 1973. **41**: p. 155.

23. L.Keddie, J., *Film formation of latex.* Mater Sci Eng R, 1997. **21**: p. 101-70.

24. S. S. Voyutskii, N.M.F., R. M. Panich, *Filtration of emulsions.* Izvestiya Vysshikh Uchebnykh Zavedenii, Khimiya i Khimicheskaya Tekhnologiya, 1958. **2**: p. 170-9.

25. Calvert, P., *Freeforming of polymers.* Curr. Opinion Solid State & Mater. Sci., 1998. **3**: p. 585-88.

26. Jacobs, P.F., *Rapid Prototyping & Manufacturing, Fundamentals of Stereolithography*. 1992: Society of Manufacturing Engineers.

27. Leong, K.F., et al., *Fabrication of porous polymeric matrix drug delivery devices using the selective laser sintering technique.* Proc Inst Mech Eng H, 2001. **215**: p. 191?01.

28. Vozzi, G.F., Christopher J.; Bianchi, Francesca; Ahluwalia, Arti; Bhatia, Sangeeta., *Microfabricated PLGA scaffolds: a comparative study for application to tissue engineering.* Materials Science & Engineering, C: Biomimetic and Supramolecular Systems, 2002. **C20**(1-2): p. 43-47.

29. T. H. Ang, F.S.A.S. D. W. Hutmacher.; Y. S. Wong; J. Y. H. Fuh.;X. M. Mo; H. TLoh.;E. Burdet; S. H. Teoh, *Fabrication of 3D chitosan hydroxyapatite scaffolds using a robotic dispensing system.* Materials Science & Engineering, C: Biomimetic and Supramolecular Systems, 2002. **C20**(1-2): p. 35-42.

30. R. Landers, A.P., U. Huebner, H. John, R. Schmelzeisen, R. Muelhaupt, *Fabrication of soft tissue engineering scaffolds by means of rapid prototyping techniques.* ournal of Materials Science, 2000. **37**(15): p. 3107-16.

31. Hench, L.L., *Biomaterials: a forecast for the future.* Biomaterials, 1998. **19**(16): p. 2529-43.

32. L.G. Cima, J.P.V., C. Vacanti, D.E. Ingber, D. Mooney and R. Langer, *Tissue engineering by cell transplantation using degradable polymer substrates.* J Biomech Eng, 1991. **113**: p. 143–151.

33. Hulbert, J.J.K.a.S.F., *Application of porous ceramics for the attachment of load bearing internal orthopedic applications.* J Biomed Mater Res, 1971. **2**: p. 161–168.

34. M. C. Wake, C.W.P., Jr and A. G. Mikos, *Pore morphology effects on the fibrovascular tissue growth in porous polymer substrates.* Cell Transplant, 1994. **3**: p. 339–343.

35. D. J. Mooney, L.G.C., R. Langer, L. Johnson, L. K. Hansen, D. E. Ingber and J. P. Vacanti, *Principles of tissue engineering and reconstruction using polymer-cell constructs.* Mater Res Soc Symp Proc, 1992. **252**: p. 345.

36. C. S. Chen, M.M., S. Huang, G. M. Whitesides and D. E. Ingber, *Geometric control of cell life and death.* Science, 1997. **276**: p. 1425–1428.

37. K.E. Healy, D.T.a.J.E.K., *Osteogenic cell attachment to biodegradable polymers.* Mater Res Soc Symp Proc, 1992. **252**: p. 109.

38. K.B. McClary, T.U.a.D.W.G., *Modulating fibroblast adhesion, spreading and proliferation using self-assembled monolayer films of alkylthiolates on gold.* J Biomed Mater Res, 2000. **50**(3): p. 429–439.

39. Martins-Green, M., *Dynamics of cell-ECM interactions*, in *Principles of tissue engineering*, R.S.L. R. P. Lanza, J. P. Vacanti, Editor. 2000, Academic Press: San Diego. p. 33–56 [Chapter 4].

40. LeGeros, R.Z.L.a.J.P., *Calcium phosphate biomaterials: preparation, properties, and biodegradation*, in *Encyclopedia handbook of biomaterials and bioengineering part A: materials*, D.J.T. D. L. Wise, D. E. Altobelli, M. J. Yaszemski, J. D. Gresser and E.R. Schwartz, Editor. 1995, Marcel Dekker: New York. p. 1429–1463.

41. J. P. Vacanti, M.A.M., W. M. Saltzman, A.J. Domb, A. Peter-Atayde and R. Langer, *Selective cell transplantation using bioabsorbable artificial polymers as matrices.* J Pediatr Surg, 1988. **23**(1): p. 3–9.

42. A. G. Mikos, G.S., M. D. Lyman, D. E. Ingber, J. P. Vacanti and R. Langer, *Prevascularization of porous biodegradable polymers.* Biotechnol Bioeng, 1993. **42**: p. 716–723.

43. Brekke, J.H., *A rationale delivery of osteoconductive proteins (A review).* Tissue Eng, 1996. **2**: p. 97.

44. B.L. Seal, T.C.O., A. Panitch, *Polymeric Biomaterials for Tissue and Organ Regeneration.* Mater. Sci. Eng. R, 2001. **34**: p. 147-230.

45. K.A. Athanasiou, G.G.N., C.C. Agrawal, *Sterilization, toxicity, biocompatibility, and clinical applications of polylactic acid/polyglycolic acid copolymers.* Biomaterials, 1996. **17**: p. 93-102.

46. C.M. Agrawal, G.G.N., K.A. Athanasiou, *Fabrication and characterization of PLA-PGA orthopaedic implants.* Tissue Eng., 1995. **1**: p. 241-252.

47. J.M. Brady, D.E.C., R.A. Miller,G.C. Battistone, *Resorption rate, route of elimination, and ultrastructure of the implant site of polylactic acid in the abdominal wall of the rat.* J Biomed Mater Res, 1973. **7**: p. 55-166.

48. Williams, D.F., *Some observations on the role of cellular enzymes in the in vivo degradation of polymers*, in *Corrosion and degradation of implant materials*, A.A. B.C. Syrett, Editor. 1979, American Society for Testing and Materials: Philiadelphia, PA. p. 61-75.

49. J.O. Hollinger, J.P.S., *Restoration of bone discontinuities in dogs using a biodegradable implant.* J. Oral. Maxillofac. Surg., 1987. **45**: p. 594-600.

50. C.M. Agrawal, J.B., J.D. Heckman, B.D. Boyan, *Protein release kinetics of a biodegradable implant for fracture non-unions.* Biomaterials, 1995. **16**: p. 1255-1260.

51. J.D. Heckman, B.D.B., T.B. Aufdemorte, J.T. Abbott, *The use of bone morphogenetic protein in the treatment of non-union in a canine model.* J. Bone Joint Surg. (Am), 1991. **73**: p. 750-764.

52. Vunjak-Novakovic G, M.I., Obradovic B, Treppo S, Grodzinsky AJ, Langer R, Freed LE., *Bioreactor cultivation conditions modulate the composition and mechanical properties of tissue-engineering cartilage.* J Orthop Res, 1999. **17**: p. 130-138.

53. Freed LE, V.-N.G., Langer P., *Cultivation of cell-polymer cartilage implants in bioreactors.* J Cell Biochem, 1993. **51**: p. 257-264.

54. Freed L, M.J., Nohria A, Emmanual J, Mikos AG, Langer R., *Neocartilage formation in vitro and in vivo using cells cultured on synthetic biodegradable polymers.* J Biomed Mater Res, 1993. **27**: p. 1-23.

55. Athanasiou KA, K.D., Schenck RC., *Biodegradable implants for the treatment of osteochondral defects in a goat model.* Tissue Eng, 1997. **3**: p. 363-374.

56. Klompmaker J, J.H., Veth RP, de Groot JH, Nijenhuis AJ, Pennings AJ., *Porous polymer implant for repair of meniscal lesions: A preliminary study in dogs.* Biomaterials, 1991. **12**: p. 810-816.

57. J.A.M. Ramshaw, J.A.W.V.G., *Collagen-based biomaterials.* Biotechnol. Genet. Eng. Rev., 1995. **13**: p. 335-382.

58. Friess, W., *Collagen: biomaterial for drug delivery.* Eur. J. Pharmaceut. Biopharmaceut., 1998. **45**: p. 113-136.

59. W.J. LaRochelle, K.S., N. Atabey, et al., *Heparan sulfate proteoglycan modulates KGF signaling through interaction with both ligand and receptor. Biochemistry.* Biochemistry, 1999. **38**: p. 1765-1771.

60. J. H. Brauker, V.E.C.-B., L. A. Martinson, J. Crudele, W. D. Johnston and R.C. Johnson, *Neovascularization of synthetic membranes directed by membrane microarchitecture.* J Biomed Mater Res, 1995. **29**(12): p. 1517–1524.

61. N. Wang, J.P.B.a.D.E.I., *Mechanotransduction across the cell surface and through the cytoskeleton.* Science, 1993. **260**: p. 1124–1127.

62. H. Lo, M.S.P.a.K.W.L., *of controlled release biodegradable foams by phase separation.* Tissue Eng, 1995. **1**: p. 15–28.

63. Zhang, P.X.M.a.R.Y., *Synthetic nano-scale fibrous extracellular matrix.* J Biomed Mater Res, 1999. **46**(1): p. 60–72.

64.G. Mikos, G.S., S.M. Leite, J.P. Vacanti and R. Langer, *Laminated three-dimensional biodegradable foams for use in tissue engineering.* Biomaterials, 1993. **14**(5): p. 323–330.

65. C.E. Holy, M.S.S.a.J.E.D., *Engineering three-dimensional bone tissue in vitro using biodegradable scaffolds: investigating initial cell-seeding density and culture period.* J Biomed Mater Res, 2000. **51**(3): p. 376–382.

66. A.G. Mikos, A.J.T., L.A. Czerwonka, Y. Bao, R. Langer, D.N. Winslow and J.P. Vacanti, *Preparation and characterization of poly(-lactic acid) foams.* Polymer, 1994. **35**: p. 1068–1077.

67. Mikos AG, S.G., Vacanti JP, Langer RS, Cima LG., *Biocompatible polymer membranes and methods of preparation of three-dimensional membrane structures*, in *US Patent No. 5,514,378*. 1996.

68. R.C. Thomson, M.J.Y., J.M. Power and A.G. Mikos, *Fabrication of biodegradable polymer scaffolds to engineer trabecular bone.* J Biomater Sci-Polym E, 1995. **7**(1): p. 23–38.

69. D.F. Baldwin, M.S.a.N.P.S., *The role of gas dissolution and induced crystallization during microcellular polymer processing: a study of poly(ethylene terephthalate) and carbon dioxide systems.* J Eng Mater-T ASME, 1995. **117**(1): p. 62–74.

70. D.J. Mooney, D.F.B., N.P. Suh, J.P. Vacanti and R. Langer, *Novel approach to fabricate porous sponges of poly(-lactic-co-glycolic acid) without the use of organic solvents.* Biomaterials, 1996. **17**(14): p. 1417–1422.

71. V.P. Shastri, I.M.a.R.L., *Macroporous polymer foams by hydrocarbon templating.* Proc Natl Acad Sci USA, 2000. **97**(5): p. 1970–1975.

72. K. Whang, C.K.T., G. Nuber and K.E. Healy, *A novel method to fabricate bioabsorbable scaffolds.* Polymer, 1995. **36**(4): p. 837–842.

73. K.E. Healy, K.W., C. H. Thomas, *Method of fabricating emulsion freeze-dried scaffold bodies and resulting products*. 1998, US Patent No. 5,723,508.

74. L.D. Harris, B.S.K.a.D.J.M., *Open pore biodegradable matrices formed with gas foaming.* J Biomed Mater Res, 1998. **42**(3): p. 396–402.

75. Mikos, L.L.a.A.G., *The importance of new processing techniques in tissue engineering.* MRS Bull, 1996. **21**(11): p. 28–32.

76. Cowsar, D.R., *Introduction to controlled release*, in *Controlled Release of Biologically Active Agents*, A.C.T.a.R.E. Lacey, Editor. 1974, Plenum Press: New York. p. 1-13.

77. Patwardhan, S.A. and K.G. Das, *An overview of controlled-release technology*, in *Controlled-release technology - Bioengineering aspects*, K.G. Das, Editor. 1983, Wiley: New York.

78. Lee, V.H.-L. and J.R. Robinson, *Methods to achieve sustained drug delivery- The physical approach: oral and parenteral dosage forms*, in *Sustained and controlled release drug delivery systems*, J.R. Robinson, Editor. 1983, Dekker: New Yrok. p. 123-209.

79. Yum, S.I. and R.M. Wright, *Drug delivery system based on diffusion and osmosis*, in *Controlled Drug Delivery, Vol. 2: Clinical Applications*, S.D. Bruck, Editor. 1983, CRC Press: Boca Raton. p. 65-87.

80. Zeoli, L.X. and A.F. Kydonieus, *Physical methods of controlled release*, in *Controlled Release Technology*, K.G. Das, Editor. 1983, Wiley: New York.

81. Baker, R.W., ed. *Controlled release of biologically active agents*. 1987, John Wiley & Sons: New York.

82. Heller, I., *Use of polymers in controlled release of active agents*, in *Controlled Drug Delivery - Fundamentals and Applications*, J.R.R.V.H.-L. Lee, Editor. 1987, Dekker: New York. p. 179-212.

83. Shah, A.C., *Design of oral sustained release drug delivery system: In-vitro/In-vivo considerations*, in *Oral Sustained Release Formulations: Design and Evaluation*, A. Yacobi and E. Halperin-Walega, Editors. 1988, Pergamon Press: New York. p. 35-56.

84. Fan, L.T. and S.K. Singh, *Controlled release - A quantitative treatment*. 1989, New York: Springer-Verlag. 1-166.

85. Chien, Y.W., *The use of biocompatible polymers in rate-controlled drug delivery systems.* Pharm. Technol., 1985. **May**: p. 50-66.

86. Crank, J., *The Mathematics of Diffusion*. 1975, Oxford: Clarendon Press.

87. Higuchi, T., *Mechanism of sustained action medication.* J. Pharm Sci., 1963. **52**: p. 1945.

88. Yolles, S. and M.F. Sartori, *Erodible matrices*, in *Controlled Release Technologies: Methods, Theory, and Applications*, A.F. Kydonieus, Editor. 1980, CRC Press: Boca Raton. p. 1-6.

89. Jalil, R.U., *Biodegradable poly (lactic acid) and poly (lactide-co-glycolide) polymers in sustained drug delivery.* Drug Dev. Ind. Pham., 1990. **16**(16): p. 2353-2367.

90. Hopfenberg, H. and H.L. Frisch, *Transport of organic micromoleculess in amorphous polymers.* J. Polym. Sci., 1969. **7**: p. 405-409.

91. **Vrentas,** J.S., C.M. Jarzebski, and J.L. Duda, *A Deborah number for diffusion in polymersolvent systems.* A.I.Ch.E. J., 1976. **21**: p. 894-901.

92. Vrentas, J.S., C.M. Jarzebski, and J.L. Duda, *Diffusion in polymer solvent systems.* J. Polym. Sci., Polym. Phys., *1977*(15): p. 441-457.

93. Ingber, D.E., *Mechanical, chemical determinants of tissue development*, in *Principles of tissue engineering*, R.S.L. R. P. Lanza, J. P. Vacanti, Editor. 2000, Academic Press: San Diego. p. 101–10 [Chapter 9].

94. Vacanti, J.P. and R. Langer, *Tissue engineering: the design and fabrication of living replacement devices for surgical reconstruction and transplantation.* Lancet (suppl. I), 1999. **354**: p. 32.

95. *Beyond the Petri dish.* Nature Biotechnology, 2004. **22**: p. 151-152.

96. Mirjam, M.P.Z., et al., *Epithelial polarity and tubulogenesis in vitro.* Trends Cell Biol., 2003. **13**(4): p. 169.

97. Hutmacher, D.W., *Scaffold design and fabrication technologies.* J. Biomater. Sci. Polymer Ed., 2001. **12**(1): p. 107.

98. McDonald, J.A., C.J. Ryall, and D.I. Wimpenny, *Rapid Prototyping Casebook.* 2001: Professional Engineering Publishing Limited.

99. Leong, K.F., C.M. Cheah, and C.K. Chua, *Solid freeform fabrication of three-dimensional scaffolds for engineering replacement tissues and organs.* Biomaterials, 2003. **24**(13): p. 2363.

100. Landers, R., et al., *Fabrication of soft tissue engineering scaffolds by means of rapid prototyping techniques.* J. Mater. Sci., 2000. **37**(15): p. 3107.

101. Dhariwala, B., E. Hunt, and T. Boland, *Rapid Prototyping of Tissue-Engineering Constructs, Using Photopolymerizable Hydrogels and Stereolithography.* Tissue Engineering, 2004. **10**(9/10): p. 1316-1322.

102. Merrill, E.W., *Biomedical compositions preparation of intraocular lenses*, in *PCT Int. Appl*. 1993.

103. S.M. Malmonge, C.A.Z., W.D. Belangero, *Biomechanical and histological evaluation of hydrogel implants in articular cartilage.* Braz. J. Med. Biol. Res., 2000. **33**(3): p. 307-12.

104. Janes, K.A. and M.J. Alonso, *Depolymerized chitosan nanoparticles for protein delivery: preparation and characterization.* J. Appl. Polymer. Sci., 2003. **88**: p. 2769.

105. Eisenberg, C.A. and D.M. Bader, *The establishment of the mesodermal cell line QCE6: a model system for cardiac cell differentiation.* Circ Res., 1996. **78**: p. 205-216.

106. Rueb, C.J. and C.F. Zukoski, *Viscoelastic properties of colloidal gels.* Journal Of Rheology, 1997: p. 197-218.

107. Alexandridis, P. and T.A. Hatton, *Poly(ethylene oxide)-poly(propylene oxide)-poly(ethylene oxide) block copolymer surfactants in aqueous solutions and at interfaces: thermodynamics, structure, dynamics, and modeling.* Colloids Surf. A, 1995. **96**(1-2): p. 1.

108. Nijenhuis, K.t., *Thermoreversible Networks: Viscoelastic Properties and Structure of Gels*, in *Advances in Polymer Science*. 1997, Springer: Berlin, Germany.

109. Channell, G.M. and C.F. Zukoski, *Shear and compressive rheology of aggregated alumina suspensions.* Aiche Journal, 1997. **43**(7): p. 1700-1708.

110. Firth, B.A. and R.J. Hunter, *Flow Properties of Coagulated Colloidal Suspensions III. The Elastic Floc Model.* Journal of Colloid and Interface Science, 1976. **57**(2): p. 266-275.

111. Buscall, R., I.J. McGowan, and C.A. Mumme-Young, *Rheology of Weakly Interacting Colloidal Particles at High Concentration.* Faraday Discuss. Chem. Soc., 1990. **90**: p. 115-127.

112. Buscall, R., et al., *Scaling Behavior of the Rheology of Aggregated Networks formed from Colloidal Particles.* Journal of the Chemical Society Faraday Transactions I, 1988. **84**(12): p. 4249-4260.

113. Buscall, R. and I.J. McGowan, *Sedimentationoand Viscous Flow of a Weakly Flocculated Concentrated Dispersion.* Faraday Discussions of the Chemical Society, 1983. **76**: p. 277-90.

114. Potanin, A.A. and W.B. Russel, *Fractal Model of Consolidation of Weakly Aggregated Colloidal Dispersions.* Physical Review E, 1996. **53**(4): p. 3702-09.

115. Buscall, R., et al., *The Rheology of Strongly-Flocculated Suspensions.* Journal of Non-Newtonian Fluid Mechanics, 1987. **24**: p. 183-202.

116. Buscall, R., J.I. McGowan, and A.J. Morton-Jones, *The rheology of concentrated dispersions of weakly attracting colloidal particles with and without wall slip.* Journal of Rheology, 1993. **37**(4): p. 621-641.

117. Sonntag, R.C. and W.B. Russel, *Elastic Properties of Flocculated Networks.* Journal of Colloid and Interface Science, 1987. **116**(2): p. 485-489.

118. Shih, W.-H., et al., *Mechanical Properties of Colloidal Gels.* Materials Research Society Symposium Proceedings, 1989. **155**: p. 83-92.

119. Shih, W.-H., et al., *Scaling Behavior of the Elastic Properties of Colloidal Gels.* Physical Review A, 1990. **42**(8): p. 4772-4779.

120. Shih, W.Y., W.-H. Shih, and I.A. Aksay, *Elastic and Yield Behavior of Strongly Flocculated Colloids.* Journal of the American Ceramic Society, 1999. **82**(3): p. 616-24.

121. Guo, J.J. and J.A. Lewis, *Aggregation Effects on the Compressive Flow Properties and Drying Behavior of Colloidal Silica Suspensions.* Journal of the American Ceramic Society, 1999. **82**(9): p. 2345-58.

122. Heyes, D.M., D.J. McKenzie, and R. Buscall, *Rheology of Weakly Flocculated Suspensions: Experiment and Brownian Dynamics Simulation.* Journal of Colloid and Interface Science, 1991. **143**(2): p. 303-16.

123. I. V. Yannas, E.L., D. P. Orgill, E. M. Skrabut and G.F. Murphy, *Synthesis and characterization of a model extracellular matrix that induces partial regeneration of adult mammalian skin.* Proc Natl Acad Sci USA, 1989. **86**: p. 933.

124. Matthew, J. *Polymeric Gels as Cell Encapsulation Materials for Tissue Engineering*. 2001 [cited; Available from: http://www.ecs.umass.edu/hamilton/2001/matthew_julie.htm.

125. Smay, J.E., et al., *Colloidal Inks for directed assembly of 3-D periodic structures.* Langmuir, 2002. **18**: p. 5429.

126. Li, Q. and J.A. Lewis, *Nanoparticle Inks for Directed Assembly of Three-Dimensional Periodic Structures.* Advanced Materials, 2003. **15**(19): p. 1639-1643.

127. Corporation, D., *Chemical Properties of Selected Polymers*. 2000.

128. Schade, A.N., Toshiyuki; Takeuchi, Hirofumi; Hino, Tomoaki; Kawashima, Yoshiaki., *Aqueous colloidal polymer dispersions of biodegradable DL-lactide/glycolide copolymer as basis for latex films: a new approach for the development of biodegradable depot systems.* International Journal of Pharmaceutics, 1995. **117**(2): p. 209-17.

129. Bottaro, D.P., A. Liebmann-Vinson, and M.A. Heidaran, *Molecular signaling in bioengineered tissue microenvironments.* Ann NY Acad Sci., 2002. **961**(143-153).

130. Hubbell, A., *Bioactive biomaterials.* Curr Opin Biotechnol, 1999. **10**: p. 123-129.

131. Saltzman, W.M., *Growth factor delivery in tissue engineering.* MRS Bull, 1996. **21**: p. 62-65.

132. Edelman, E.R., M.A. Nugent, and M.J. Karnovsky, *Perivascular and intravenous administration of basic fibroblast growth factor: vascular and solid organ deposition.* Acad Sci US A, 1993. **90**(5): p. 1513-7.

133. Langer, R., *New methods of drug delivery.* Science, 1990. **249**(4976): p. 1527-33.

134. Boontheekul, T. and D.J. Mooney, *Protein-based signaling systems in tissue engineering.* Curr Opin Biotechnol., 2003. **14**(5): p. 559-565.

135. Bodmeier, R., X. Guo, and O. Paeratakul, *Process and Formulation Factors Affecting the Drug Release From Pellets Coated With Ethylcellulose Pseudolatex Aquacoat*, in *Aqueous Polymeric Coatings for Pharmaceutical Dosage Forms*, J.W. McGinity, Editor. 1997, Marcel Dekker Inc: New York. p. 55-80.

136. Maejima, T. and J.W. McGinity, *Influence of film additives on stabilizing drug release rates from pellets coated with acrylic polymers.* Pharm Dev Tech., 2001. **6**(2): p. 211-221.

137. Baldwin, S.P. and W.M. Saltzman, *Materials for protein delivery in tissue engineering.* Adv. Drug Delivery Rev., 1998. **33**: p. 71-86.

138. J. E. Smay, et al., *Colloidal Inks for directed assembly of 3-D periodic structures.* Langmuir, 2002. **18**: p. 5429-5437.

139. Peniston, Q.P. and E.L. Johnson, *Pocess for depolymerization of chitosan*. 1975: U.S.

140. Cheng, A., et al., *A simple mechanical mixer for small viscous lipid-containing samples.* Chemistry and Physics of Lipids, 1998. **95**(1): p. 11.

141. Xu, Y. and Y. Du, *Effect of molecular structure of chitosan on protein delivery properties of chitosan nanoparticles.* Int. J. Pharm., 2003. **250**(1): p. 215.

142. Ross, R., *Platelet derived growth factor.* Annu Rev Med., 1987. **38**: p. 71.

143. Heldin, C.H., et al., *Binding of different dimeric forms of PDGF to human fibroblasts: evidence for two separate receptor types.* EMBO J., 1988. **7**: p. 1387.

144. Hart, C.E., et al., *Two classes of PDGF receptor recognize different isoforms of PDGF.* Science, 1988(240): p. 1529-1531.

145. Soma, Y., K. Takehara, and Y. Ishibashi, *Alteration of the chemotactic response of human skin fibroblasts to PDGF by growth factors.* Exp. Cell. Res., 1994. **212**: p. 274.

146. Crouch, M.F., et al., *Activation of Endogenous Thrombin Receptors Causes Clustering and Sensitization of Epidermal Growth Factor Receptors of Swiss 3T3 Cells without Transactivation.* The Journal of Cell Biology, 2001. **152**(2): p. 263-273.

147. Mi, F.L., et al., *Kinetic Study of Chitosan-Tripolyphosphate Complex Reaction and Acid-Resistive Properties of the Chitosan-Tripolyphosphate Gei Beads Prepared by in-Liquid Curing Method.* J Polym Sci Polym Phys, 1999. **37**: p. 1551-1564.

148. Calvo, P., C. Remuñán-López, and J.L. Vila-Jato, *Novel hydrophilic chitosan-polyethyleneoxide nanoparticles as protein carriers.* J Appl Poly Sci, 1997(63): p. 125-132.

149. Keddie, J.L., *Film formation of latex.* Mater Sci Eng R, 1997. **21**: p. 101-70.

150. Eckersley, S.T. and A. Rudin, *Mechanism of Film Formation From Polymer Latexes.* Journal of Coatings Technology, 1990. **62**(780): p. 89-100.

151. Onions, A., *Films from Water-Based Colloidal Dispersions.* Manufacturing Chemist, 1986(March): p. 55.

152. Cho, M.I., W.L. Lin, and R.J. Genco, *Platelet-derived growth factor-modulated guided tissue regenerative therapy.* J Periodontol, 1995. **66**(6): p. 522–530.

153. England, J., *Stabilization and Release Effects of Pluronic F127 in Protein Drug Delivery.* J. Undergrad. Sci., 1999. **5**(2): p. 17-24.

154. Beaman, J.J., *Solid Freeform Fabrication: a new direction in maufacturing*. 1997, Dordrecht; Boston: Kluwer Academic Publishers.

155. Luiz Carlos Junqueira, J.C., Robert O Kelley, Luis Carl Junqueira, *Basic Histology*. 9th edition ed. 1998: McGraw-Hill/Appleton & Lange. 494.

156. Junqueira, L.C. and J. Carnerio, *Basic Histology*. 10 ed.

157. Schauer, A. and W. Becker, *The Sentinel Lymph Node Concept*. 2004: Springer Verlag.

VITA

Baojun Xie

Candidate for the Degree of

Doctor of Philosophy

Thesis: COLLOIDAL GEL AND ITS APPLICATION IN TISSUE ENGINEERING

Major Field: Chemical Engineering

Biographical:

Personal Data: Baojun Xie was born on October 15 , 1974, in Baoji ,China and is the son of Yupeng Xie and Daxi Wang.

Education: He attended Tsinghua University, China in July and received Bachelor of Engineering in Chemical Engineering with polymer specialty in 1996. Then he entered Chinese Academy of Sciences, China and received his first Master of Sciences degree in Organic Chemistry and Polymer Science in July, 1999. Unpon entering Oklahoma State University, he obtained his second Master of Science degree in Chemical Engineering at in August, 2003. At last he completed the requirements for the Ph. D. degree in Chemical Engineering at Oklahoma State University in December, 2005.

Experience: He joined in China Petroleum & Chemical Corporation (SinoPEC), Jinling Company as a R&D engineer in September, 1999 and latter was promoted to department manager. He used to work in Sciperio and Vaxdesign as a full time intern.

Name: Baojun Xie Date of Degree: December, 2005

Institution: Oklahoma State University Location: Stillwater, Oklahoma

Title of Study: Colloidal Gel and Its Application in Tissue Engineering

Pages in Study: 94 Candidate for the Degree of Doctor of Philosophy

Major Field: Chemical Engineering

Scope and Method of Study: Three dimensional, porous polymer scaffolds are fabricated by direct writing of colloidal gels. This work focuses on both the processing of colloidal gel and assembly of the scaffold structures as well as characterization of cytotoxicity and protein release kinetics. Specifically, rheological and elastic properties of the colloidal gels are probed as a function of solids loading and binder concentration. Porous scaffolds are characterized by optical and electron microscopy. *In vitro* studies include cell mortality after six weeks culture on passive scaffolds, model protein release profiles from scaffolds, and quantitative measurement of protein activity upon release from the scaffolds by chemotaxis.

.

Findings and Conclusions: The polymer colloidal gels formulated with acrylic latex particles and Pluronic F127 copolymer binder have pseudoplastic with yield stress rheology. Increases in solids loading and Pluronic concentration cause increased viscosity, elastic modulus, and yield stress. The rheology and rapid recovery of yield allow for flow through a deposition nozzle of the direct write tool and rapid setting of the extrudate to maintain the deposited structure. Scaffolds with a wide variety of porosity are fabricated. Because of the aqueous and low temperature nature of the process, bioactive molecules such as proteins are readily incorporated into the scaffold either in their original form or encapsulated in chitosan nanoparticles and subsequently released without denaturation and in a controlled fashion. Protein release rate is dependant on both the degree of coalescence of the scaffold material and the molecular weight of the chitosan nanoparticles. Protein inclusion and subsequent release is demonstrated using BSA and PDGF-BB. The scaffolds fabricated are non-cytotoxic as confirmed by QEC6 cell culture. Heterogeneous scaffolds with localized regions of dissolved species are demonstrated to illustrate the capability to assembly scaffolds with functional gradients or segregated zones.

ADVISOR'S APPROVAL: _____James E. Smay_____